Agricultural Water Management 305 (2024) 109128

Contents lists available at ScienceDirect

Agricultural Water Management

journal homepage: www.elsevier.com/locate/agwat

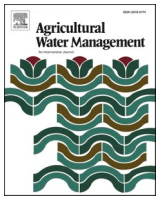

Assessment of irrigation water use for dry beans in center pivots using ERA5 Land climate variables and Sentinel 2 NDVI time series in the Brazilian Cerrado

Laura De La Guardia *, Jarbas Honorio de Miranda, Ana Claudia dos Santos Luciano

University of São Paulo (USP), Luiz de Queiroz College of Agriculture (ESALQ), Piracicaba, SP, Brazil

ARTICLE INFO

Keywords:
Water resources
Dry beans
Irrigation water use
Dry season agriculture

ABSTRACT

The Brazilian Cerrado is a vital agricultural region, yet its expansion often overlooks the high climate risks posed by the prolonged dry season, particularly from June to September when water demand surges, causing low-flow conditions. Recent studies highlight significant water deficits between May and October, making irrigation water use (IWU) crucial for policymakers and managers. This study estimates IWU for dry beans grown under center pivots during the dry season in the state of Mato Grosso, Brazil, a leading agricultural producer with 309,372 km^2 of agricultural land. Mato Grosso relies heavily on irrigation from April to October for bean cultivation. We used NDVI time series from Sentinel-2A data from 2019 to 2023 to classify dry beans areas based on t-SNE and k-means cluster classification. The individual NDVI time series for the dry season for each pivot was divided based on the peak NDVI values to analyze phenological parameters- such as duration, start and end of the season- to assess water needs from April to September. ERA-5 Land climate data provided daily reference evapotranspiration (ETo) and precipitation (P), which were used to compute the crop's water requirement. Irrigation depth (D) was estimated using a water balance equation incorporating crop coefficients (Kc) and daily irrigation needs adjusted for efficiency. The analysis shows that dry-season irrigation in the Cerrado primarily replenishes soil moisture, often leading to inefficient water use. From 2019–2023, IWU increased significantly, with the model showing a strong correlation ($R^2 = 0.92$) to reported accumulated irrigation depth for center pivot during the dry season. However, the model underestimated needs from May to July and overestimated in August, with a bias of −21.88 mm. The North subregion, benefiting from favorable conditions, accounted for 43 % of the state's IWU. The study provides valuable insights into IWU trends, supporting strategic decisions and resource allocation, while offering a cost-effective method for real-time IWU estimation.

1. Introduction

In the last decades, Brazil has won and holds the title of one of the most competitive agricultural producers and exporters of oilseeds, cereal, fruits, and animal protein in the world (CONAB, 2023; Bigolin and Talamini, 2024). The country has remained the largest soybean producer, responsible for one-third of global production (Rattis et al., 2021). Brazil is also the third largest global corn producer, and it is expected to reach first place in the upcoming years (Colussi et al., 2023). Similarly, Brazil is one of the largest producers of edible dry beans worldwide (Heinemann et al., 2016; Silva and Flake, 2019), as well as the largest consumer since dry beans are a primary source of the Brazilian diet, approximately 16.0 kg/person/year, making beans a key player of the nation food security (da Silva and Wander, 2018). To reach such high levels of production, a double cropping system is used in most of the country to grow soy and corn. In this system, soy is sown in September/ October, and after its harvest in January/February, corn is sown in the same plot (Bigolin and Talamini, 2024). Beans are grown in three crop seasons, depending on the region (da Silva and Wander, 2018). The first crop season goes from November through February. The second crop season, more common nationwide, goes from March through June, and the third crop season, which grows in the dry winter months, from May through September (Silva and Flake, 2019). Some regions in the country not only hold the double cropping system of soy and corn but also the third crop season of beans within the same agricultural year. One of these regions is the Brazilian Cerrado, which

* Corresponding author.
E-mail addresses: lauradlg@usp.br (L. De La Guardia), analuciano@usp.br (A.C. dos Santos Luciano).

https://doi.org/10.1016/j.agwat.2024.109128
Received 1 August 2024; Received in revised form 16 October 2024; Accepted 21 October 2024
Available online 31 October 2024

accounts for 45 % of the national agricultural area (Ferreira et al., 2023), and it plays an important role as a non-stop agricultural production center for the nation's food supply and the world.

Agricultural production, however, has been affected worldwide by climate change and rising food demand, increasing irrigation demand to hold up production (Ma et al., 2022). This reality is not foreign to Brazil. There has been a statistical reduction in rainfall for the period of 1978–2015 in intensive industrial agricultural areas of the country (Pousa et al., 2019). The scenario does not seem to improve, since studies have shown that most regions of Brazil are likely to experience a decrease in mean annual precipitation, reducing evaporation and water availability (da Silva Tavares et al., 2023). Not surprisingly, the average yearly growth of irrigated areas had increased from 130 to 216 thousand hectares per year in the last two decades (ANA, 2021), making Brazil one of the ten countries with the largest area equipped for irrigation worldwide (FAO, 2020). Center pivot has been the most adopted irrigation system to irrigate various crops (Althoff and Rodrigues, 2019). Official reports from the National Water and Sanitation Agency (ANA) estimate that water withdrawals for irrigation were 1083.6 m^3/s in 2017 (ANA, 2019a), dropping to 965 m^3/s - 941 m^3/s according to updated studies (ANA, 2021). ANA's approach is designed for large-scale, national estimates. Their water consumption coefficients are expressed in liters per second per hectare (L/s/ha) and assume continuous irrigation for 24 hours a day based on crop water requirements provided by FAO guidelines (ANA, 2019b). This level of generalization is useful for broad policy and resource management decisions but may not capture the localized, crop-specific variations in water demand, particularly during the dry season. The discrepancies in irrigation area reported in ANA's 2017 and 2021 reports also reflect the complexity of estimating water use at such a broad scale, with values dropping from 1083.6 m^3/s to around 965–941 m^3/s due to updates in agricultural area estimates and coefficient refinements. To the best of our knowledge there are no official numbers of water used by irrigation system and by crop season, and the time needed to publish the results hinders water management. Considering that a drier climate could intensify water conflicts by threatening water security for multiple water users, quantitative knowledge of irrigation resources is essential for stakeholders and users in charge of managing agricultural services and food production (Brocca et al., 2018).

Despite the impressive growth, the country aims to keep expanding agricultural areas. It is estimated that the Brazilian Cerrado has the highest potential for agricultural expansion, with approximately 70 % of its 204 million hectares capable of development (Francisco and Kappes, 2012). Analysis of the climate water balance of the Brazilian Cerrado indicates that regions located in the transition between the Cerrado and Amazon biome have a higher potential for water availability (Ferreira et al., 2023). These regions include part of the states of Maranhão, Tocantins, and Mato Grosso. These states have undergone agricultural intensification thanks to the incorporation of new technologies (Pousa et al., 2019) and management practices, such as adoption of irrigation systems and conservation agricultural practices that include crop rotation, crop diversification, and the use of cover crops. Agricultural expansion has been accomplished under the umbrella of the Brazilian Forest Code, by which farmers need to keep 20 % of native vegetation on their property (Colman et al., 2022). Nevertheless, studies indicate that irrigation is still one of the most efficient ways to increase food production in established agricultural lands in the Cerrado (Althoff and Rodrigues, 2019), but at the same time, it is challenging to implement due to the limited supply of freshwater. Currently, nearly 54 % of the pivots in Brazil are in the Brazilian Cerrado, with a higher frequency in Minas Gerais, Goiás, Bahia, and Mato Grosso. The last two states have a higher average size of center pivot, with 120.92 Ha and 105.08 Ha for Mato Grosso and Bahia, respectively (Althoff and Rodrigues, 2019). Considering the substantial expansion of farming and irrigated areas, where two or more crops a year are common (Pimenta et al., 2021), monitoring becomes challenging due to the lack of data and reference information (ANA, 2021).

The emergence of new remote sensing tools and techniques has brought an opportunity to overcome challenges of crop mapping and monitoring, both at the field scale and large scale (Bégué et al., 2018). The spectral imaging offered a non-invasive and rapid measurement of plants or crop canopies as the reflected light changes according to the leaf's physical and biochemical properties (Stamford et al., 2023). The main advantage of orbital remote sensing products has been their integration into free cloud web services that allow their application for earth science research. For instance, the Google Earth Engine (GEE) platform makes use of cloud-based digital processing to house a large repository of publicly available geospatial datasets (e.g., satellite and aerial images, weather forecast, land cover, etc.), allowing efficient and friendly access (Gorelick et al., 2017). Users can access and control data through an Internet-accessible application programming interface (API) that enables the application of computational mathematical models, machine learning operations, and the computation of vegetation indices (VI) such as the Normalized Difference Vegetation Index (NDVI), Leaf Area Index (LAI), among others. Several Brazilian studies have used this free platform to analyze different orbital data products to map and quantify environmental degradation and changes in land cover (Silva et al., 2022), and analyze trends across the Western (Pimenta et al., 2021), Northeast and Center region (Lewis et al., 2022; Silva et al., 2023, 2024). There are different earth observation sources with which it is possible to compute vegetation indices, e.g., MODIS, Sentinel-2, and Landsat. However, their effectiveness depends on the research objective, as they have either high spatial or temporal resolutions and different spectral resolutions. In the specific case of agricultural landscapes, where field size can cover a couple of hectares, a spatial resolution of tens of meters is necessary (Guzinski et al., 2023). Song et al. (2021) evaluated Landsat (7&8), Sentinel-1 (A&B), Sentinel 2 (A&B), and MODIS for crop type mapping of corn and soybean in the United States, proving that Landsat, Sentinel-2 or Sentinel-1, could achieve 94.8–96.8 % accuracy, while the coarse-resolution of MODIS produced 92 % of accuracy (Song et al., 2021). Recent studies assessed the effectiveness of different imagery collections to identify vegetation types in the Brazilian Cerrado and indicated the benefits of using Sentinel-2 over Landsat-8 in terms of accuracy and spatial resolution (Lewis et al., 2022).

Data acquired by optical sensors have been widely used to identify not only irrigated areas (Peña-Arancibia et al., 2014; Zaussinger et al., 2019) but also to characterize seasonal dynamic of vegetation at local, regional, and global scales (Rodigheri et al., 2023). The application of vegetation and water indices from multi-spectral band ratios, such as the NDVI, has been effectively used to monitor crop dynamics (Ma et al., 2022). Despite the challenges of cloud cover, noisy data, and lower temporal resolution (D'Odorico et al., 2015), NDVI have proved effective in representing crop growth rates when processed correctly (Ji et al., 2021). Oliveira et al. (2024) evaluated the efficiency of vegetation indices from Sentinel-2A/ MSI and Unmanned Aerial Vehicles (UAVs) to study the spectral response through the different phenological stages of common bean in an experimental irrigated field in the Midwest region of Brazil. Their study pointed out that VI from Sentinel-2A/MSI can help manage bean crops throughout their growth. The PCA comparison with UAV data showed a good match ($R^2 = 0.667$) and low error (RMSE = 0.12). NDVI and MCARI indices were particularly useful for predicting crop productivity, with a correlation of $r = 0.82$ and RMSE values of 330 and 329 kg/ha, respectively, thus promoting the potential use of geotechnologies for crop monitoring (de Oliveira et al., 2024). Different algorithms, publicly available, have been developed to extract phenological parameters such as sowing and harvest dates from NDVI time series (Rodigheri et al., 2023) based on mathematical models or threshold-based approaches that use reference values of vegetative activity (USGS, 2018). For instance, Ji et al. (2021) derived the daily NDVI for corn fields based on the 8-day NDVI using spline interpolation. They identify the date when the NDVI curve began to increase at the bottom of the valley as the start day, and the data when the NDVI reached the

bottom of the valley after the single NDVI corn peak as the end date (Ji et al., 2021). Rodigheri et al. (2023) performed a comparative analysis of six different phonologic metrics algorithms using data from 1500 fields distributed across the central area of Brazil. Their study revealed that although the algorithms produced significantly different phenological estimates, the best estimates were obtained with TIMESAT and phenex, with R greater than 0.7, followed by the Earth Australia tools package (DEA) despite the higher sensitivity to data sources. Nevertheless, the authors pointed out that double cropping added a level of complexity that no method was able to automatically identify it (Rodigheri et al., 2023). Therefore, with proper processing, phenological information can be extracted from remote sensing VI.

Irrigation requirement, defined as the amount of water provided to crops when precipitation does not entirely satisfy the evapotranspiration demand, is commonly estimated by water balance models (Jalilvand et al., 2019). The consumptive use of water by irrigated crops is usually quantified using the crop coefficient procedure, where the grass reference evapotranspiration (ETo) is multiplied by an empirical crop coefficient (K_c) (Allen, 2000), resulting in crop evapotranspiration (ETc). The Kc coefficient corrects ETo to account for the plant development, climate, and management factors (Marin et al., 2019), and it can be obtained from FAO-56 reference values (Allen, 2000). ETo can be computed with the Penman-Monteith (P-M) equation when information is available through the FAO 56 monograph, FAO 56 (P-M) ETo, or it can be acquired from remote sensed or model-based estimates from products from MODIS or ERA5-Land. Due to the limited coverage of weather stations in Brazil, with often missing data and a density of only 0.001 stations per 100 km^2, when the recommended is 6.3 stations per 100 km^2, gridded weather databases are recommended (Duarte and Sentelhas, 2020). ETc is also computed from different satellite products. For instance, MOD16A2 Version 6.1, from the MODIS catalog, provides an 8-day dataset of ETc at 500-meter pixel resolution based on the logic of the P-M equation, which includes inputs of daily meteorological reanalysis data, together with vegetation properties, albedo, and land cover from MODIS (Running et al., 2024). Nevertheless, since surface conditions change from day to day over agricultural fields, daily temporal resolution is preferred for robust estimates (Guzinski et al., 2023). Duarte and Sentelhas (2020) evaluated the effectiveness of using the Brazilian interpolated data system, DailyGridded, with a resolution of 0.25º, and NASA/POWER dataset, with a resolution of 0.5º, for estimating maize yields in Brazil. Their study computed the confidence index (C) for both datasets showing that DailyGridded data has a better performance ($0.55 < C < 0.99$) than NASA/POWER ($0.09 < C < 0.99$) for all weather variables and time scales (Duarte and Sentelhas, 2020). However, the temporal coverage of DailyGridded is from January 1961 to July 2020. ERA5-Land, produced by the Copernicus Climate Change Service (C3S), provides high-resolution precipitation and other climate variables with a resolution of 0.1° at an hourly temporal resolution by combining satellite information and ground measurements (Rolle et al., 2021). Studies based on satellite data were able to obtain favorable results to assess water use for irrigation at farm and basin levels, especially for the most drought-prone areas of the country (Folhes et al., 2009; Santos et al., 2020; de Sousa Junior et al., 2022). Therefore, there is room to apply this methodology over large irrigation areas.

Based on the relevance of the agricultural areas in the Brazilian Cerrado, the pursuit of increasing production is understandable. However, it is known that farming expansion is commonly assessed based on total annual precipitation and does not consider the high climate risk associated with the length and intensity of the dry season (Rattis et al., 2021). Due to the remarkably high seasonality of the region, the occurrence of events characterized by low-flow conditions related to water demand increase from June until September (Althoff et al., 2021). Moreover, a recent analysis of spatiotemporal variability of annual precipitation and evapotranspiration also depicts the severity of water deficit in the region during the drought months from May to October (Ferreira et al., 2023). The dry season also coincides with heightened wildfire occurrences (WWF-Brasil, 2024), an increase in electricity demand, and a rise in the cost of hydroelectric generation (DW Brasil, 2024). Therefore, knowledge of irrigation water use (IWU) applied in each growing season can provide valuable insights for managers and policy makers (Massari et al., 2021). For these reasons, this paper aims to estimate the IWU by center pivots during the dry season alone. Since in Brazil, policies and management practices are usually applied at the state level, this study focuses on one of the states with the highest development potential in the Cerrado: Mato Grosso. The locally applied irrigation depth is computed by center pivot during the dry season, from April to October, from 2019 to 2023. This study will focus on edible beans, which are crucial for food security, and calculate locally applied irrigation depth from April to October between 2019 and 2023. Accumulated irrigation depth was compared against individual field scale irrigation reported by farmers in four municipalities of Mato Grosso. Climate variables for the FAO water balance equation are sourced from ERA-5 Land, and phenological stages and crop classification are derived from the NDVI time series from Sentinel-2A. By quantifying IWU, this study provides essential data for optimizing water resource allocation during the dry season. It helps policymakers design efficient irrigation strategies, reducing environmental impacts and supporting more sustainable agricultural expansion. Additionally, the findings contribute to developing energy demand scenarios and improving understanding of the food-water-energy nexus, enabling better resource management and long-term planning for the region's sustainability and resilience.

2. Study site

The state of Mato Grosso in Brazil (Fig. 1) has 900,000 km^2, and its 309,372 km^2 of agricultural area covers the Amazon biome (humid forest) in the north, Pantanal biome (tropical wetland) in the South, and the Cerrado biome (tropical savanna) in the center. According to the Köppen classification, the climate is hot, semi-humid to humid, with a dry winter season from May to October (Brown et al., 2013). The annual precipitation in the north exceeds 2000 mm, while in the South, it reaches 1000 mm. The state's annual rainfall ranges from 1300 to 2300 mm. The length of the dry season also varies, from 3 months in the north to up to 5 months in the South (Arvor et al., 2014; Zhang et al., 2021). From 1991–2020, the mean rainfall for May, June, July, August, and September is 53.4 mm, 19.7 mm, 10.2 mm, 13.2 mm, and 50.5 mm, respectively. In the last 30 years, there has been a tendency for a reduction in rainy days by month, decade after decade. The number of rainy days for May, June, July, August, and September are 4 days (SD=1.3), 1 day (SD=1.0), 1 day (SD=0.7), 1 day (SD=1.3), and 5 days (SD=1.6), respectively (Noronha Marcuzzo et al., 2012).

The state alone has been one of the leading agricultural producers of soy and corn in the world and has the most center pivot increment in the 2010–2017 period (175 % growth), consolidating itself as an essential Brazilian irrigation center (de Albuquerque et al., 2020). Mato Grosso has the highest potential for expansion of irrigated areas (ANA, 2021), due to the high freshwater volume from numerous rives, aquifers, and the planet's largest floodable area called Pantanal (Ferrarini et al., 2019). Besides the predictability of double cropping in the state (Rattis et al., 2021) during the agricultural year (September to August), the third harvest of edible beans has been consistent in Mato Grosso (CONAB, 2016). In Mato Grosso, beans constitute the main grain cultivated during the dry season, winning the name of "irrigated beans" as it occurs largely under irrigation, with first plantings starting in April and harvests until October (Wander, 2007; ANA, 2021). Economic studies showed the profitability of the third harvest in the state. For instance, in 2015, 29,272 ha of irrigated beans were planted in the state, reaching a yield of 2052 kg ha^{-1} (da Silva and Wander, 2018).

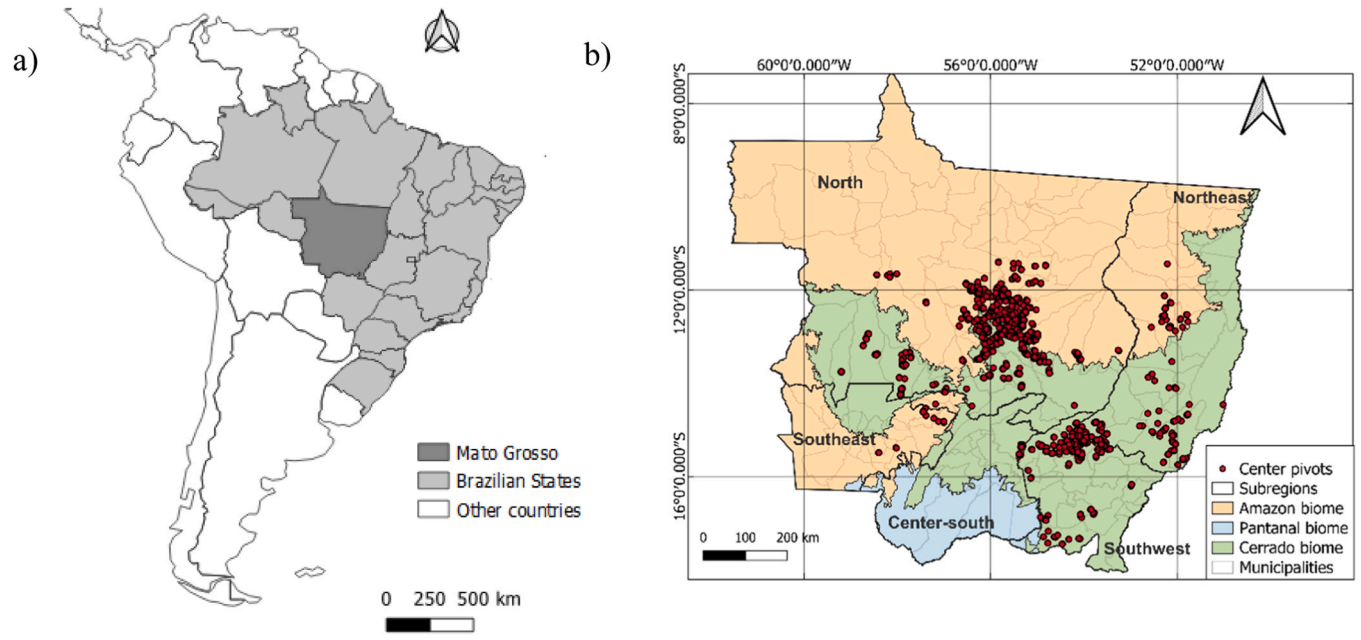

Fig. 1. a) Location of Mato Grosso in Brazil, and b) location of center pivots in Mato Grosso. A total of 73 % of center pivots are in the Cerrado biome, while the remaining 27 % are in the transition to the Amazon biome.

3. Material and methods

3.1. Datasets

3.1.1. Climate datasets

The fifth generation of European ReAnalysis, hereafter referred as ERA5-Land, is a component of the Copernicus Climate Change Service (C3S). Reanalysis provides a numerical description of the recent climate by combining past short-range weather forecast models with observations through data assimilation (Hersbach, 2016; Service/ECMWF, 2023). ERA5-Land produces hourly high-resolution information of a total of 50 variables describing the water and energy cycles over land globally at a 9 km spatial resolution (Muñoz-Sabater et al., 2021). Hourly climate data was downloaded through the Application Programming Interface (API) of the European Centre for Medium-Range Weather Forecasts (ECMWF), from 2019/01/01–2023/12/31.

3.1.2. Ancillary datasets

The center pivot boundary maps from the Brazilian National Water Agency (ANA) and MapBiomas were used to compute the irrigation requirement for each pivot. ANA's pivot map is available as shapefile in their webpage (Pereira Guimarães et al., 2023). MapBiomas irrigation collection 3 for 2022, available as a tiff file, was produced on visual interpretation of imagery acquired from Landsat 5, Landsat 8, and Sentinel 2 A/ 2B satellites, and an adapted U-Net architecture, together with high-resolution images from Google Earth and reference maps from ANA (Rudorff and Oliveira, 2023). In Mato Grosso were found 1034 pivots from ANA's records, covering an area of 125,449 ha, and 381 pivots in MapBiomass covering 120,972 ha. All pivots have an identifier number and are classified in five sub-regions: north, northeast, southwest, southeast, and central south. The unification of center pivot boundaries in Mato Grosso from ANA and MapBiomas is presented as geopackage file in the supplementary data.

3.1.3. Sentinel imagery

Sentinel 2 Multispectral Instrument Level-2A images were used through the Google Earth Engine (GEE) cloud computing platform to compute the Normalized Difference Vegetation Index (NDVI). Level-2A refers to orthoimage atmospherically corrected capturing the surface reflectance. The spatial resolution for the bands 2 (492 nm), 3 (560 nm), and 4 (665 nm), used in the NDVI computation, is 10 m. The combined constellation revisit time is five days near the Equator (Gascon et al., 2017). The image collection was clipped using the center pivot geometry. Then, a cloud-free time series of NDVI for the period of January 2019 to December 2023 was created.

3.2. NDVI time series processing

The NDVI time series of each pivot, comprising the data from 2019 to 2023, was downloaded from GEE, and processed in Google Colab. The first step of processing was standardizing the data format to later compile the files in a single DataFrame. All operations mentioned hereafter were applied for each pivot-ID. Even though the cloud effect on the NDVI was removed in the GEE preprocessing, many random factors affect NDVI time series, making the data irregular (Hird and McDermid, 2009). There is no best de-noise technique since it greatly varies according to the vegetation type and NDVI data source (Geng et al., 2014), but the literature pointed out techniques widely used in crop NDVI series. In our case, since the presence of clouds was high in the north and northeast regions near the Amazonia, the time series had sudden oscillations and consecutive missing values, e.g., ten days, making difficult the application of common de-noise techniques. A rolling window with a size of three days was applied to obtain the maximum NDVI value ($NDVI_{max,\ i}$). When the difference between the current NDVI, $NDVI_i$ and $NDVI_{max,\ i}$, was higher than 0.3, the observation was filtered from the DataFrame. Each time series was interpolated using a polynomial method of second-order at a 3-day scale to fill existing gaps. Subsequently, the Best Index Slope Extraction (BISE) algorithm was then used to remove outliers and sudden decreases from the time series since it retains the most valuable elements of an NDVI profile (Viovy et al., 1992). To reduce remaining noise reduction, the NDVI time series must be smoothed. Among popular smoothing methods, the Savitzky-Golay (SG) filtering procedure was proved to better characterize the signals from crops (Ji et al., 2021) due to its ability to preserve higher NDVI values and account for negatively-biased noise, keeping the original tendency of the series (Hird and McDermid, 2009). Thus, considering that Sentinel 2 A has a five-day temporal resolution, the SG filter was applied to all time series with a window size of 5 and a

polynomial degree of 2.

Since most of the information available concerning crop management is published by crop season, the NDVI time series data was categorized into crop season within the agricultural year, starting from September 15th, and ending on the same day of the upcoming year. To facilitate numerical operations, a new variable called 'Day of season' (DOS) was added to keep track of the NDVI series continuously. For instance, the date '2019–09–13' is equivalent to DOS=363 of Crop season 2018, and '2019–09–16' is equivalent to DOS=1 of Crop season 2019.

As it was mentioned before, cloud presence on consecutive days diminished the effectiveness of de-noise methods. To handle remaining errors, the coefficient of variance (CV) was computed by pivot ID and by crop season (pivot-season). CV values smaller than 0.1 indicated a straight-line behavior that was incongruent with vegetation development. Thus, pivot-season in that range was filtered from the DataFrame.

3.3. Classifying center pivot with growing crops

As explained in Section 3.1.3, center pivot geometry was used to clip the image collection of Sentinel 2, assigning the pivot ID as a parameter and computing the NDVI at pivot level. However, it is not known if the pivots were active during the crop season. Moreover, it has yet to be discovered in which harvest or for which crop pivots were used. Previous studies analyzed the time series of vegetation indexes and determined representative vegetative development profiles on irrigated areas in the country, portraying the dynamic of Brazilian agriculture (do Nascimento Bendini et al., 2019; Kuchler et al., 2020; de Sousa Junior et al., 2022).

Fig. 2-a) shows the vegetation development profile for center pivots in fields with the third crop harvest. The peak in vegetation development occurs within the month of July. To determine if pivots were used or not for growing crops, the mean NDVI of July was computed for each pivot ID by crop season (pivot-season). During the five years of records, 2019–2023 (five crop season, 2018–2022), NDVI values ranged from 0.15 to 0.5 along May through September. An NDVI threshold of 0.25 was obtained in other studies in Brazil (Santos et al., 2020), and was used to assign the status of the pivots for each year. Pivots with NDVI lower than 0.25 in the month of July were classified as "without growing crop." Pivot-season in this category were filtered from the dataset.

3.4. Crop classification

Due to the vast diversity of biome and weather, there is a crop calendar for each region in Brazil. The Ministry of Agriculture, Livestock and Food Supply, through its Secretariat of Animal and Plant Health, establishes a sanitary void of soybean in June and July to prevent Asian soybean rust and a sanitary void of cotton from October to November. According to the crop calendar of Mato Grosso (Fig. 3), the period of the third harvest required for the development of dry beans overlaps with the late development of corn, mid and late development of cotton, and the growing of some cover crops. Therefore, the months of May and June provide the best window to distinguish crops since dry beans would be an early development, thus, in a low range of the NDVI, while other crops would be in a higher NDVI range.

The median NDVI for each pivot-season, only for May and June, was computed. The result was subjected to K-means clustering, an unsupervised classification method that can identify groups of similar data points known as clusters (Brown et al., 2013). The number of groups was tested with the silhouette score (Hayasaka, 2022), which summarizes within-cluster and between-cluster variation. A silhouette coefficient close to 1 indicates that the clustering algorithm can efficiently divide the data into separated clusters. The results were compared with the records of nine pivots with dry beans located in the municipalities of Sinop and Sorriso, and three pivots with cotton, located in the municipalities of Nova Ubirata. All municipalities mentioned before are in the North region of Mato Grosso. Since irrigated cotton fields are not within the scope of this study, pivot-season classified as cotton were dropped from the DataFrame. The K-means clustering method was applied to the median NDVI of May and June by pivot-season. A group number, n=6, obtained the best silhouette score (s= 0.67).

Considering that each irrigated field is subject to management practices such as those responding to local weather influence, and crop selection, among others, there is a high dimensionality in the time series looking at the state level. One recent popular technique for dimensionality reduction is the t-distributed stochastic neighborhood embedding (t-SNE), which has been applied in numerous fields, especially where ground truth is unknown (Linderman and Steinerberger, 2019). The t-SNE is commonly used to simplify the identification of clusters as it focuses on preserving the pairwise similarities between data points (van der Maaten and Hinton, 2008), giving it an advantage over techniques like Principal Component Analysis (PCA). The t-SNE technique was applied together with the K-means cluster and later compared with Fig. 2-a) to classify the irrigation fields by pivot-season that follow a third harvest profile.

3.5. Determination of phenological parameters

The variation in sowing dates can occur at individual field levels due to climatic, legal (prescribed sanitary period), and socio-economic constraints (Zhang et al., 2021); the sowing date was determined for each pivot-season. A set of techniques and algorithms available to compute the Land Surface Phenology (LSP) information. Among them, the Digital Earth Australia (DEA) function *xr_phenology* computes several LSP statistics which describe the lifecycle of plants by seasons in a practical manner (Rodigheri et al., 2023). The package was developed in Python, and the script is available in a well-documented GitHub repository (Geoscience Australia, 2024). The script uses the NDVI time series of the growing season and identifies the peak of the crop season, the day of the year (DOY) corresponding to it, POS, and value of NDVI at the peak of crop season (VPOS), and. The algorithm then uses the POS to split the time series into two periods: greening (DOY<POS) and senescence (DOY>POS). The DOY of the start of season (SOS) and the DOY of the end of season (EOS), can be estimated in two ways: selecting the first

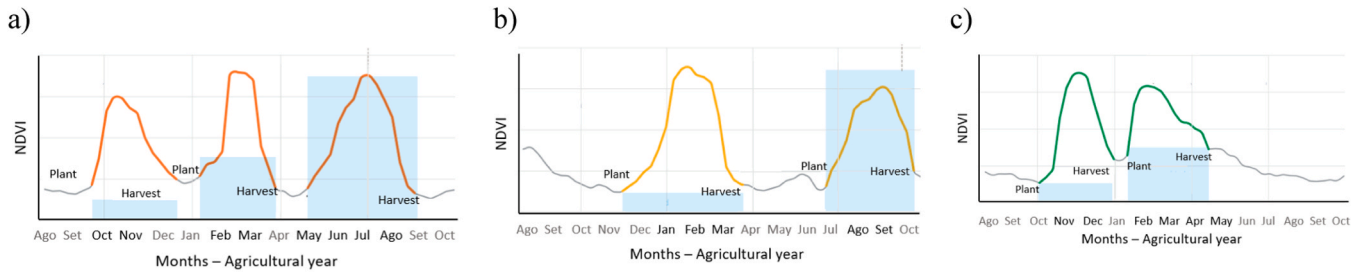

Fig. 2. Schematic representation of typical vegetation development profiles for center pivots within a crop season: a) three consecutive crop seasons, b) double-cropping, c) two consecutive crop seasons. The blue shaded area represents the schematic water requirement. Retrieved from ANA (2021).

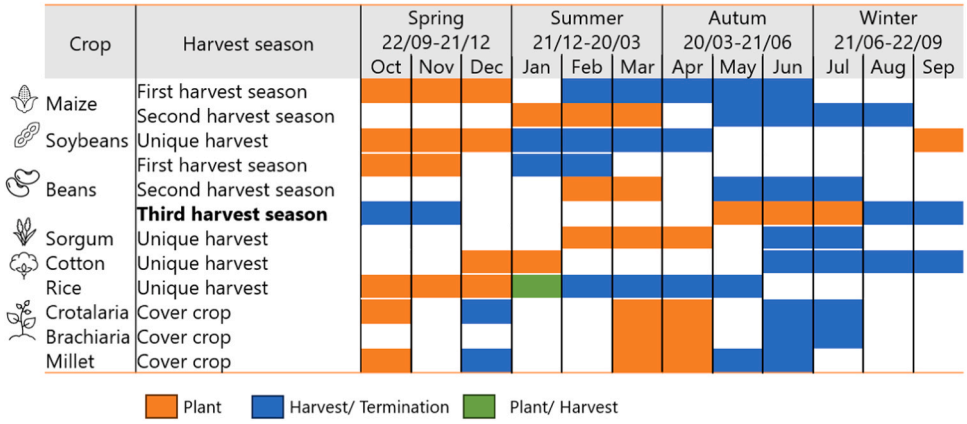

Fig. 3. Crop calendar of Mato Grosso adapted from (Conab, 2022).

positive slope of the greening side, or the median value of the curve positive slopes on the greening side. EOS can be estimated as the last negative slope on the senescing side of the curve or the median value of the negative slope. The duration of the season is computed as EOS-SOS. The algorithm was developed considering one harvest per year. Thus, its applicability for double cropping generates confusion in the algorithm (Rodigheri et al., 2023). Therefore, the original DEA function was adjusted in a customized Python script to consider only the third crop season of dry beans. Even though it follows the same logic, it uses pivot-season from the Data frame as index instead the coordinates from an Xarray data set. The former will be explained in Section 3.7 Data manipulation.

3.6. Daily precipitation and evapotranspiration

The two main climate variables used in this study were precipitation, P, and ETo. To obtain daily precipitation, hourly precipitation available in ERA5 Land was aggregated summing data from 1:00 h to 0:00 h in each day. Precipitation variables do not include fog, dew or the precipitation that evaporates in the atmosphere before it lands at the surface of the Earth. It is worth mentioning that potential evapotranspiration is also a given product in ERA5 Land, computed by making a second call to the surface energy balance assuming a vegetation type of crops and that agricultural land is a well watered. This condition is not always realistic, especially for arid and dry conditions, where the method can give unrealistic results due to the high evapotranspiration forced by dry air (Muñoz-Sabater et al., 2021). ETo is computed with the Penman-Monteith (PM) method, considering well-watered grassy surface (Allen et al., 2006) using the variables described in Table 1.

The meteorological variables needed were downloaded from the global land surface dataset of ERA5-Land reanalysis as follows:

$$ETo = \frac{0.408 \quad \Delta(R_n - G) + \gamma\left(\frac{C_n}{T_a+273}\right)u_2(e_s - e_a)}{\Delta + \gamma(1 + C_d u_2)} \tag{1}$$

$$u_2 = u_z\left(\frac{4.87}{\ln(67.8z - 5.42)}\right) \tag{2}$$

$$u_z = \sqrt{u^2 + v^2} \tag{3}$$

$$e_s = 0.6108\exp\left(\frac{17.27 \times T_a}{T_a + 237.3}\right) \tag{4}$$

$$e_a = 0.6108\exp\left(\frac{17.27 \times T_{dew}}{T_{dew} + 237.3}\right) \tag{5}$$

Table 1
Acronyms of variables used to compute reference evapotranspiration with PM method.

Variable		Units
u	10 m u-component (zonal) of wind speed	m s−1
v	10 m v-component (meridional) of wind speed	m s−1
u_z	measured wind speed z m above the ground surface	m s−1
u_2	wind speed 2 m above the ground surface	m s−1
T_{dew}	2 m dew point temperature	°C
T	2 m air temperature	°C
Ta	mean air temperature	°C
P	atmospheric surface pressure	Pa
Δ	slope of saturation vapor pressure curve	kPa °C−1
γ	psychometric constant	kPa °C−1
R_n	surface net radiation flux	MJ m−2 d−1
G	surface sensible heat flux into the soil	MJ m−2 d−1
e_a	actual vapor pressure	kPa
e_s	saturation vapor pressure	kPa
e_s-e_a	saturation vapor pressure deficit	kPa
C_p	specific heat at constant pressure, 1.013 10–3,	MJ kg−1 °C−1
ε*	latent heat of vaporization	MJ kg−1
C_n	numerator constant for the reference crop type and time step, 37	
C_d	denominator constant for the reference crop type and time step, 0.34	

$$\Delta = \frac{4098 \quad e_s}{(T_a + 237.3)^2} \tag{6}$$

$$\gamma = \frac{C_p \times P}{\varepsilon *} \tag{7}$$

In this study, the daily actual evapotranspiration, Eta, was computed following the FAO methodology (Allen, 2000):

$$ETc_i = ETo_i \times kc_i \times ks_i \tag{8}$$

where ETo and ETc are expressed in mm/day, *i* denotes the specific day, kc is a dimensionless coefficient specific for each crop and growing phase obtained from FAO-65 reference values for dry beans in dry weather, and ks is the water stress coefficient which ranges from 0 to 1. Since we are only evaluated center pivot fields, ks=1 assuming that crops are not under water stress.

3.7. Data manipulation

Climate variables for the computation of ETo, as well as precipitation, were downloaded at an hourly scale through a Python script using the ECMWF API. ERA5-Land climate data is saved as a multidimensional

array depicting variables by latitude, longitude, and time, and it is commonly saved as network common data form (NetCDF). The original dataset contains eleven variables at an hourly scale for the five years of study, for the area of Mato Grosso containing center pivots. Xarray library was used to manipulate the multidimensional arrays since its data structure uses dimensions and coordinates to enable its core metadata operations (Developers, 2014). The latitude, longitude, and time were assigned as indexes and coordinates. The ETo was computed using the mentioned above ten variables. The data array containing the variables ETo and Precipitation, was converted from hourly to daily scale.

The method "nearest" in Xarray allows the automatic finding and selection of the nearest available point in the coordinate space of the dataset (Developers, 2014). This method was used to retrieve ETo and precipitation data, originally under the latitude and longitude of the ERA5-Land grid, to match the latitude and longitude of center pivots' s centroid. In other words, the data set was reshaped to display the variables by pivot id, pivot's latitude and longitude, and time. The time dimension was changed from date format to "day of the year" (DOY) and year. The final dataset, as shown in Fig. 4, contains the variables precipitation, ETo, and pivot area stored by pivot ID (georeferenced by each pivot's centroid coordinates) and time (DOY and year). Finally, the sowing dates by pivot ID and year were added to the dataset, using the combination of the two coordinates in common: pivot ID-Year.

3.8. Estimating actual evapotranspiration and quantifying irrigation depth required

In this study, irrigation requirement is defined as the amount of water provided to crops when P does not entirely satisfy the ETc (Rolle et al., 2021). One standard procedure to compute ETc is to estimate the ETo, which describes the theoretical dynamics of water removal from land back to the atmosphere (Singer et al., 2021), and then apply the corresponding empirical crop coefficient (Kc). The Kc coefficient corrects ETo to account for the plant, climate, and management factors (Marin et al., 2019). This simplified but easily applicable method where ETc = ETo × Kc, provides an opportunity of water quantity used for irrigation without involving complex tasks.

To compute the ETc, two simplifications were made: 1) the crop planted in each center pivot during the dry season, for each year, was *Phaseolus vulgaris* (common bean), 2) each stage of phenological development (initial, crop development, mid-season and late season) follows the time window presented in the FAO guidelines (Allen, 2000). To account for the phenological stages, a new variable called "day of stage" was created to register the number of days after the sowing date. The Kc values for beans, (Kc_{ini}=0.4, Kc_{mid}=1.15 and Kc_{late}=0.35) were assigned based on the day of stage.

ERA5-Land considers P as the precipitation that lands at the surface of the Earth. For irrigation purposes, effective rainfall must be considered to evaluate if rainfall is enough to cover crops' water needs. Effective rainfall is influenced by storm intensity and duration, soil slope, texture and structure, and plant cover, among others. During dry periods, the FAO-25 guideline assumes that daily precipitation of less than 5 mm would not be considered effective as it would likely evaporate before it reaches the ground. There are different methods to compute effective rainfall (soil water balance approach, Renfro equation, and other empirical methods). However, they do not always satisfactorily suit specific local situations (Ali and Mubarak, 2017). Due to the scale of the study and field data limitations (e.g., soil type and daily soil moisture records during the irrigation period), the computation of effective rainfall is not feasible. Since the dry season in Mato Grosso has a mean precipitation of 29.4 mm and a mean number of rainy days of 2.4 days, the effect of effective rainfall, only during the dry season, is negligible. The irrigation depth (D)- or water application rate- for each pivot was calculated at a daily scale according to Eq. (9) (Frizzone et al., 2018; Santos et al., 2020), where ε indicates the water application efficiency of the center pivot, and *i* represents the time scale. ε is a measure of the fraction of the total water volume delivered to the field, which is stored in the root zone to meet the ETc needs (Irmak et al., 2011). Water losses in sprinkler irrigation need to be considered, including wind drift and evaporation of droplets (at the canopy and the soil surface). However, this field data is often not available or not measured. As a simplification, an ε of 65 %, 70 %, 75 %, and 80 % were used for all pivots to compare the theoretical D with field data. If ETc is less than the P, the water demand of the crop is met, and thus, D is zero. On the other hand, when ETc exceeds P, the difference must be satisfied through irrigation.

$$D_i = \max\left(\frac{ETc_i - P_i}{\varepsilon}, 0\right) \quad (9)$$

In summary, the entire process of computing irrigation depth can be divided into two stages (Fig. 5). The first stage is the NDVI time series smoothing process, which was used for 1) categorizing the status of irrigation fields (growing or no growing crops), 2) classifying crop and categorizing vegetation development profiles, and 3) compute LSP. In the second stage, the climate variables from ERA5-Land were used to compute the reference evapotranspiration. The results of the first stage were used to filter pivot-season that were within the scope of the study, and the LSP was used to compute the actual evapotranspiration.

4. Results and discussion

4.1. Crop classification

For pivot-season categorized with 'growing crops', irrigated fields were correctly classified according to the records of pivot-ID from the municipalities of Sorriso, Sinop and Nova Ubirata (Fig. 6), following the NDVI threshold of 0.25 from Santos et al. (2020). An accuracy assessment was conducted with field data to classify the two main crops grown in the dry season, which have different NDVI time series signatures: beans and cotton. Using the k-means cluster result, pivot-season classified as cotton were filtered from the DataFrame, as they are out of the scope of this study. Fig. 6-b) shows the NDVI time series for crop season

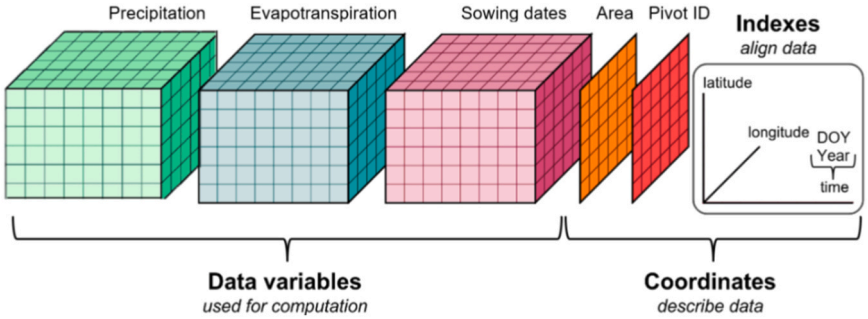

Fig. 4. Xarray data structure of the current study, adapted from (Developers, 2014).

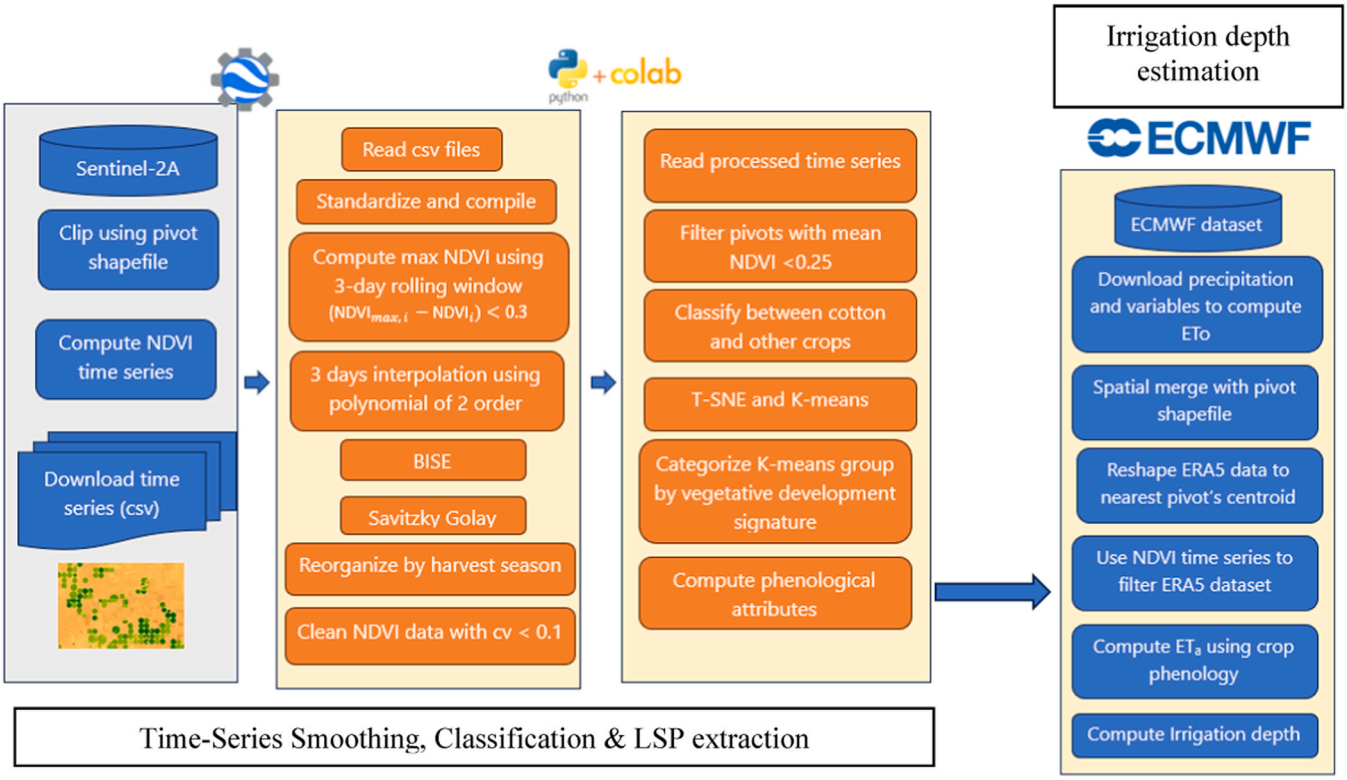

Fig. 5. Flowchart of stages of LSP extraction and climate variables integration to compute irrigation depth.

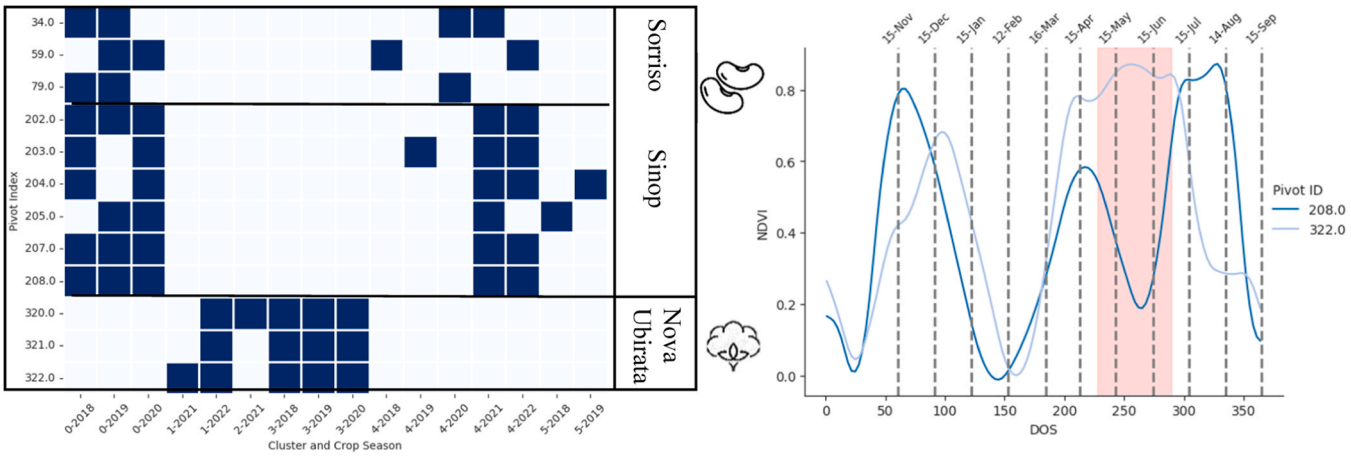

Fig. 6. a) K-mean classification by Crop season and pivot ID, b) NDVI time series of pivot ID-208 (dry beans-Sinop) and pivot ID-322 (cotton-Nova Ubirata). Red shaded area represents the values used to compute the median NDVI.

2018 of two irrigated fields: pivot ID 208 with dry beans in the municipality of Sinop and pivot ID 322 with cotton in the municipality of Nova Ubirata. Both fields show an expected behavior at the beginning of the crop season, but after February, pivot ID 322 depicts the profile of two crop seasons while pivot ID 208 follows three crop seasons.

As shown in Fig. 3, within the dry season, there are crops in different development stages. To account for that rate of change in the NDVI time series, the DataFrame was resampled, computing the mean every ten days, starting from April to September. The t-SNE was used for pivot ID, crop season, and subregion. Each t-SNE coordinates (t-SNE 1 and t-SNE 2) represent a transformed version of the original high dimensional data. t-SNE 1 and t-SNE 2 represents the direction of maximum variance, thus, closer data points indicate high similarity, while dissimilar datapoints are placed far apart in the plot (Poličar, 2023). Clusters or groups of points that form in the plot suggest that those points share common features or properties in the original data. Perplexity is another parameter that impacts how the t-SNE algorithm balances the attention between local and global structures. A low perplexity values emphasis on local structure (individual clusters), while higher values capture global structure (relationships between clusters). For this dataset, a perplexity value of 50 showed a good visualization of clusters. Fig. 7 shows the clusters formed using the 10-day mean NDVI. Observations of all regions within each cluster, indicate that their division is driven due to crop characteristics and growth rate, rather than geographical differences.

The K-means were applied to classify clusters using t-SNE 1 and t-SNE 2 with a k number of 7. It is seen in Fig. 8 that, except for group 3 and group 7, most of the irrigated fields exhibit a behavior of three crop

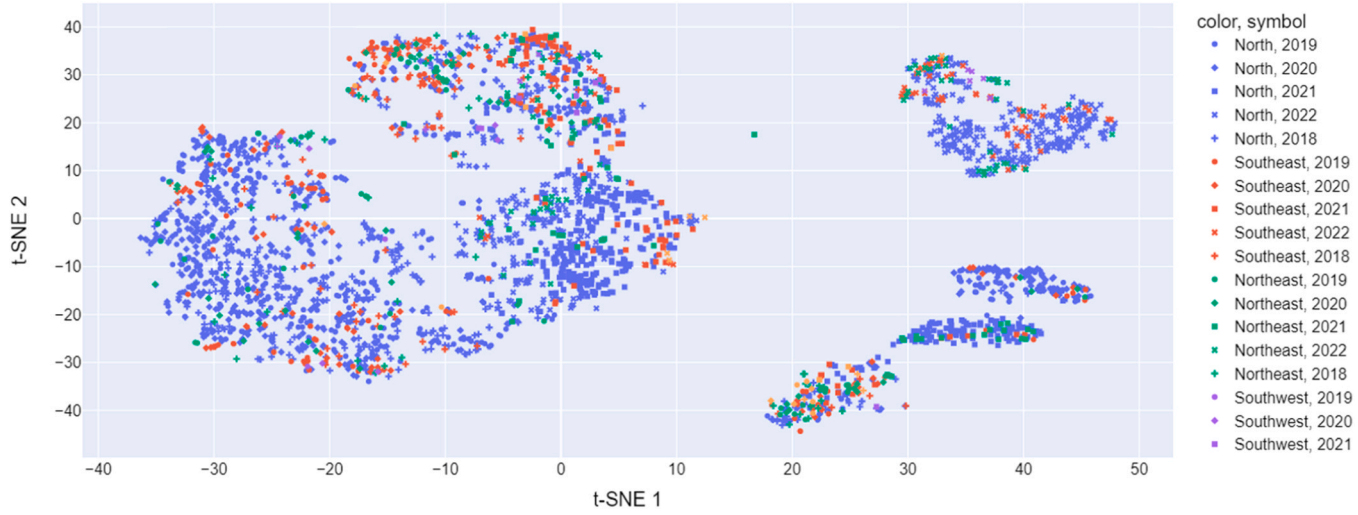

Fig. 7. t-SNE visualization of NDVI time series resampled at 10 days, classified by region and crop season. t-SNE 1 captures the most significant variation among the data points, such as the most distinct groups. t-SNE 2 captures differences within clusters, or secondary structures in the data.

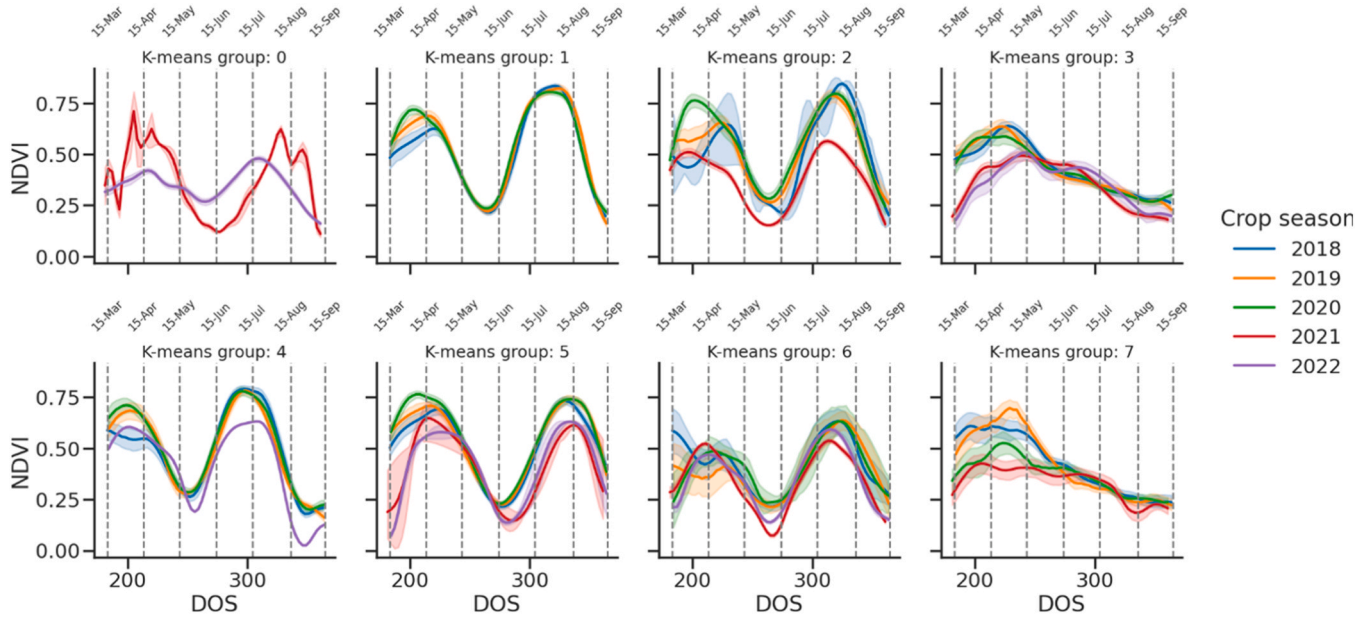

Fig. 8. NDVI times series by crop season plotted by k-means group.

harvests. Thus, pivot-season within groups 3 and 7 were dropped from the dataset. Most of the groups follows a similar pattern for all crop seasons. The most apparent disparities are found in group 2, in which crop season 2018 had a different behavior during the months of June and July which may have been caused due to weather conditions of that particular year.

4.2. Crop phenology

Phenology metrics such as the start, peak and end of the season, and duration of the season were computed. To avoid mixing other crops, pivot-season with a duration of greater than 60 days was used. The final dataset contains the phenology metrics of 714 active pivots with dry beans in Mato Grosso (Fig. 9). The wider section in the violin plot on Fig. 9 represent a higher probability of irrigated fields starting the third crop season on that day of the year.

The SOS shows variation across the years. 2018 has a broader spread, starting around DOY 130 and extending to DOY 180, indicating a later start for some observations. For SOS, the start dates are relatively consistent in 2018 but become increasingly variable in subsequent years, with 2022 showing the widest spread. Crop season 2021 presented later SOS than in other years. Crop season 2022 shows a high concentration around DOY 145. Overall, there is a trend of SOS occurring between mid-May to early June, with some yearly variations showing a slightly earlier or later start.

EOS values range broadly from DOY 200–245 (Fig. 9). EOS appears to be more concentrated around DOY 240 and 245. Crop seasons 2021, 2022 exhibit a high EOS concentration of around DOY 240. The distribution of EOS shows a significant variability, ranging from late July to early September. Due to the higher economic value of soybeans, which are grown after dry beans, extending the dry bean season is not economically viable for farmers. However, it was noticed that farmers using center pivots can begin planting earlier than rainfed systems once the sanitary void ends, even when rainfall is delayed, providing them an advantage.

The duration of the harvest seasons ranges from 60 to 110 days. In

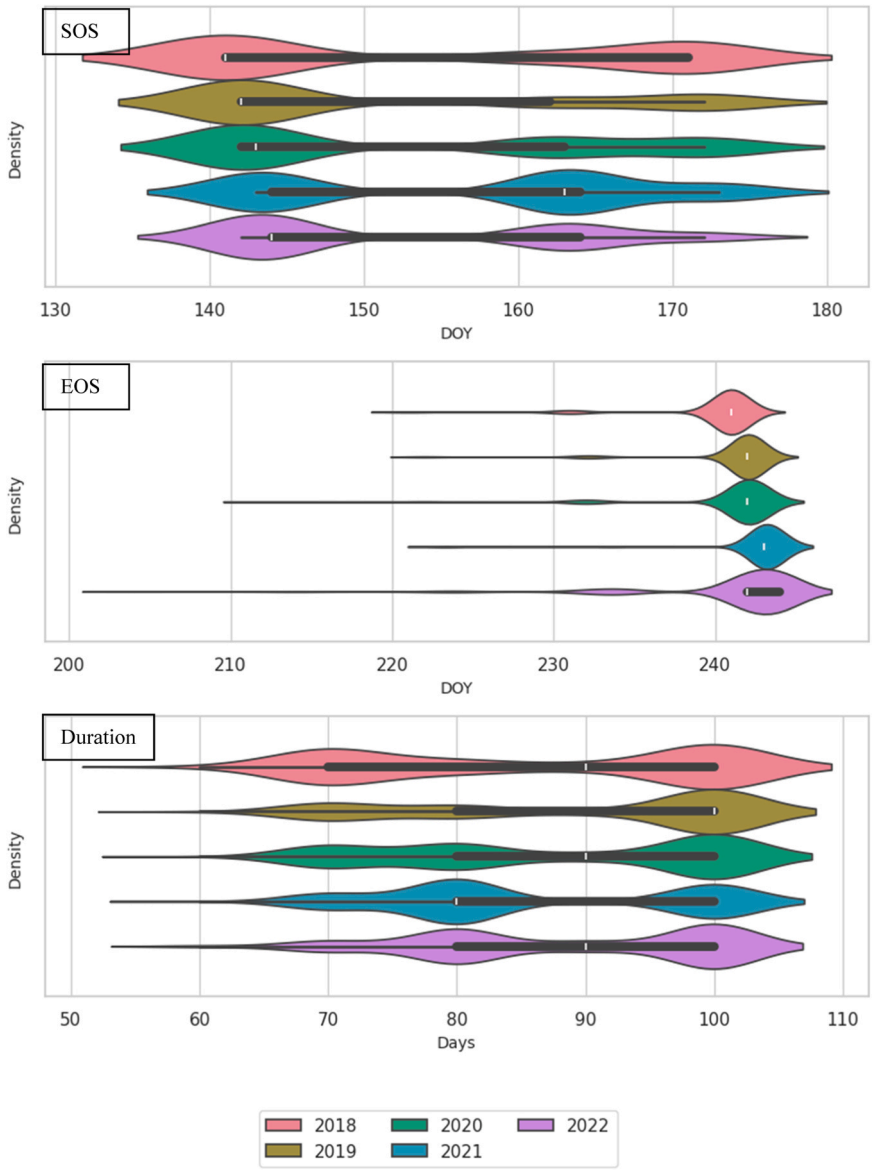

Fig. 9. Violin plot of five crop season distribution of start of the season (SOS), end of the season (EOS) and duration of the third harvest season. White dot represents the median, thick black bar in the center represents the interquartile range, and thin black line represents the rest of the distribution. The Kernel density estimation is represented on each side of the black line to represent the distribution of the data.

crop season 2018, the duration is more variable, ranging from 70 to 105 days. The duration also exhibits year-to-year variability, with 2018 and 2020 having shorter, more consistent durations, while 2021 and 2022 display longer and more variable durations. Crop season 2019, 2020, 2021, and 2022 show a more consistent duration around 80–100 days. The overall trend indicates a relatively consistent duration of the dry bean harvest, lasting between 80 and 100 days.

4.3. Irrigated area

After all filtering stages, the surface area of active pivots classified with dry beans at least one crop season from the five subregions of the state was summed by crop season (Fig. 5). As it was mentioned before, most of the pivots are in the Cerrado biome, mainly in the transition from the Cerrado to the Amazon biome (North and Northeast sub-regions), and few pivots are found in the Pantanal biome (Center-south sub-region). For irrigated fields with dry beans, approximately 27.8 %, 23.1 %, and 0.1 % are distributed in the Cerrado, Amazon, and Pantanal biome, respectively (Table 2).

Table 2
Center pivots in Mato Grosso classified with dry beans by biome.

Biome	Center pivots in Mato Grosso		Center pivots with dry beans	
	Number of pivots	Total Area (Ha)	Number of pivots	Total Area (Ha)
Amazonia	462	96,197.06	323	67,964.77
Cerrado	938	145,236.97	390	60,729.39
Pantanal	1	275.50	1	275.50
Total	1401	241,709.53	714	128,969.66

Compared to the historical dry bean crop harvest series published by the National Supply Company (CONAB) for the third crop harvest, the current approach sub-estimated the number of harvested areas for harvest 2018/2019, 2019/2020, and 2020/2021 (Table 3). This might be due to the high cloud cover or other atmospheric conditions that hindered accurate satellite detection, whereas harvest 2021/2022, and 2022/2023 had clearer conditions. In addition, continuous enhancement in the consistency and reliability of Sentinel 2 A data products

Table 3
Comparison of dry bean harvested area by crop season reported by this study and CONAB.

Mato Grosso Sub-region	Area of dry bean harvested by crop season (thousands of ha)				
	2018/2019	2019/2020	2020/2021	2021/2022	2022/2023
Central south					0.70
North	27.62	44.05	50.62	57.88	75.40
Northeast	1.80	2.53	2.39	6.08	9.14
Southeast	2.34	3.47	5.34	3.03	4.72
Southwest	0.02	0.02	0.11		0.09
Total area (thousands of hectares)	31.78	50.06	58.46	66.99	90.05
Area of dry beans harvested reported by CONAB (thousands of hectares)	46.2	53.9	67.9	64.8	78.2
Percental difference	−31.2 %	−7.1 %	−13.9 %	3.4 %	15.2 %

might contribute to better detect crop monitoring. In crop season 2021/2022, and 2022/2023, there was an overestimation of 3.4 % and 15.2 % maybe caused by management practices such as zoning irrigated fields, common on large center pivots. Farmers often divide large fields into two or more zones to better manage water usage and streamline logistics during harvest. It can be performed with one or two crops (e.g., dry beans and chia) with shorter growing periods, in which some farmers stagger the planting dates within the same field. For example, they might plant one half of the field 15–25 days after the other half. This staggered planting means the two halves of the field will have different water needs at different times. When one half of the field reaches mid-development and requires less water, the other half is at its peak water demand. This strategy allows the irrigation system to focus water on the areas that need it most during times when it's less costly to do so. However, since this dynamic was not accounted for in the initial estimations and pivots with internal dynamics were treated as standard operations, it introduced a source of uncertainty. Studies like MapBiomass Irrigation Collection 8 have identified similar challenges in managing staggered or multiple crops under center pivots. They found that staggered or multiple crops per pivot require further study and they emphasize the need for further research and detailed field data to enhance model accuracy, particularly in identifying precise planting start and end dates (Rudorff and Oliveira, 2023).

Due to the weather characteristics during the dry season explained before, it is assumed that dry bean harvested area reported by CONAB corresponds to irrigated fields, however, it does not specify the irrigation system used. National surveys might define irrigated areas differently, including additional factors that are not considered in satellite image analyses. Moreover, the algorithms and criteria used to identify center pivot systems in satellite imagery differ from those used in surveys. For example, satellite detection algorithms might miss irrigated fields with

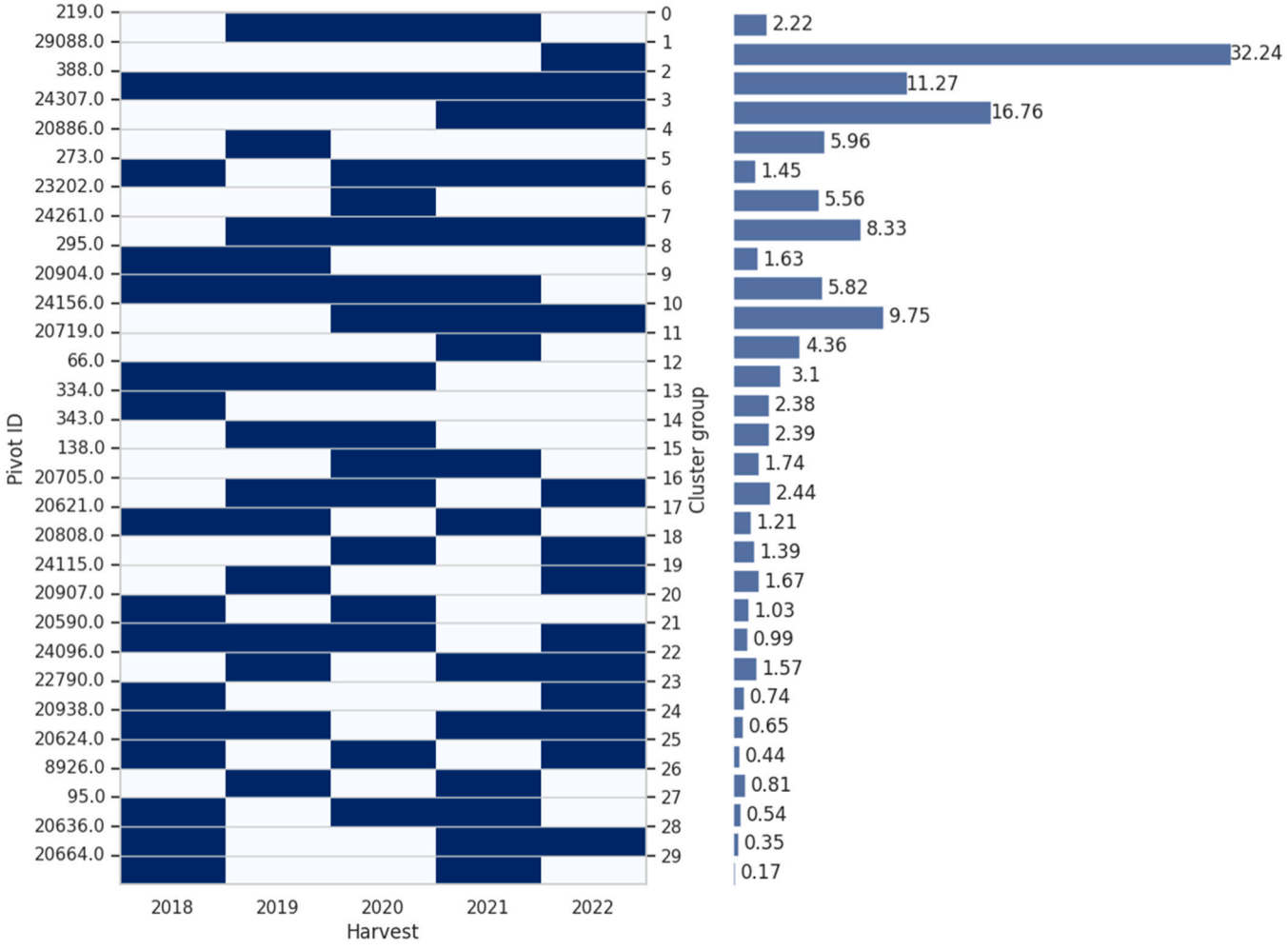

Fig. 10. Recurrence pattern of center pivot usage in the State of Mato Grosso for dry bean during the dry season. Dark blue fill represent active crop season. Sample of center pivot for each of the 29 cluster group (left). Area in thousand of hectares of center pivots within each cluster group (rigth).

different irrigation systems. Despite the difference, the methodology here presented provided near real-time estimates of active center pivots in the region.

Fig. 10 shows that it is possible to check the usage patterns of center pivots in the state. It is noticeable that there is an increment in the adoption of third harvest of dry beans (Cluster 1, e.g., 29088), congruent with publications of national reports (Conab, 2023). Due to the high cost of acquiring or leasing new areas in Mato Grosso, some farms have chosen to invest in irrigation systems to allow greater resilience to climate change (more extended droughts), as well as allow for a third harvest. Pivots within Cluster 1 added an approximate of 32.24 thousand hectares to the irrigated area of the state. Some pivots (Cluster 2, e.g., pivot ID 388) are used consistently across multiple years, while other pivots show sporadic usage (Cluster 29, e.g., pivot ID 20664). According to field visits, it was known that some pivots are no longer used or were moved due to the soil health conditions that do not make affordable continuing operations (e.g., pivot ID 24078). In other instances, the absence of dry beans during certain crop seasons does not mean that the fields remain necessarily without crop. In Brazil, the adoption of cover crops to deal with phytosanitary problems, suppression of positive photoblastic weeds, and erosion is a common practice. Particularly, the use of different species of crotalaria in succession or rotation to reduce root-lesion nematoids (Cruz et al., 2020). Since crotalaria is a bad host of nematoid, and has a high capacity of biological nitrogen fixation, it can be used alone or in combination with others cover crops, e.g., brachiaria, to promote the production of phytomass with aims to increase the yield of subsequent crops (Cherubin et al., 2022). Therefore, in some cases, to improve soil health, farm managers could opt for the use of cover crops or other crop during the dry season due to the benefits that crop rotation brings to the soil for subsequent crops.

By analyzing how the usage of pivots changes from year to year, one can identify trends or anomalies. Pivots that were only used in specific years indicate possible changes in cropping strategy or external factors affecting usage, such as crop rotation, market demands, or weather patterns. Pivots used consistently across multiple years will likely continue being used in the future. Clusters with larger areas and consistent use indicate key areas central to the agricultural and water management strategy. These clusters are likely to continue being prioritized in the future. Moreover, clusters with smaller or declining usage might indicate areas where there is potential for increased utilization if conditions change (e.g., improved irrigation infrastructure or changes in crop profitability). Likewise, fields with inconsistent usage might indicate areas more vulnerable to external factors (e.g., weather variability, soil health). Identifying these fields might allow for better risk management strategies, such as diversifying crops or improving resilience measures.

4.4. Quantification of irrigation depth

Irrigation depth was computed with Eq. (9) considering the crop water use under four different scenarios of application efficiency: 65 %, 70 %, 75 %, and 80 %. The results were compared with values reported by different studies that involve center pivots used to growth dry beans during the dry season in different localities within the Cerrado region (Table 4). Values obtained with an application efficiency of 65 % and 70 % were aligned to those found in the literature.

Fig. 11 shows that Southwest and Southeast are the subregions that require a higher accumulated depth for years 2021 and 2022, in which the third harvest was pursued. The highest individual values are seen in 2021 for the Southwest (370.7 mm) and Southeast (363.0 mm), indicating that these regions may require more water or have different irrigation practices compared to other regions. Year 2021 stands out with the highest depths in the Southeast, and Southwest, indicating a higher water need for the crops, while 2022 and 2023 have more uniform and lower depths.

Results were compared with the records of 2022 and 2023 of a center pivot (Fig. 12a) equipped with integrated monitoring and control units that stored detailed data such as system status, date of application, applied water depth, and other relevant parameters. The monthly accumulated water depth of this study estimation and the field data are showed in Fig. 13. The water applied at the beginning of the development stages surpasses the water needs of the crop. This is because, dry beans are commonly cultivated in rotation with soybean and corn. According to this system, dry beans are seeded through the residues of corn without tillage. After the second harvest season that precedes dry bean seedlings, the soil water capacity is at its lowest, closer to the wilting point. A common practice consists of replenishing the soil with consecutive irrigation events to bring the soil water capacity near to its field capacity. Records analyzed showed a median irrigation frequency of 2 days in June and July. During the mid and late season, when foliage area is high, the water applied does not meet the crop water need, to avoid increasing crop vulnerability to diseases. Variations of this practice can occur as a response to important diseases such as white mold caused by *Sclerotinia sclerotiorum* (de Abreu et al., 2022).

Nevertheless, most of the fields do not count with soil water measurement tools, and water applied by irrigation events is subject to the electricity rate schedule and configuration of the irrigation system. Between 9 PM and 6 AM, electricity rates are lower, making it cheaper to run irrigation systems. The conditions at night, such as higher humidity, lower temperatures, and reduced wind speeds, enhance water application efficiency by reducing water loss through evaporation and wind drift, ensuring more water reaches the soil. To maximize water application within this time frame, some irrigation systems use larger nozzles, which can apply more water quickly and at lower pressure, thus conserving energy (Rogers et al., 2017). As a result, the minimum water

Table 4
Irrigation depth applied (mm) and application rate (mm day^{-1}) of center pivots from different studies during winter bean harvest.

Source	Location	Altitude (m)	Temp. (°C)	Prec. (mm)	Humidity (%)	Area (ha)	Cultivar	Date	Days	Irrigation depth (mm)			App. rate (mm/d)
										Min	Max	Mean	
(Osti et al., 2019)	Tangará da Serra, Mato Grosso	440	26.1	295	70.0	67.07	Carioca	07/11/2014	91	295.1	522.2	408.7	7.00
(Soares et al., 2019)	Sorriso, Mato Grosso	386	25.0	2000	70.0	0.99	Carioca	06/10/2015	90	127.0	127.0	127.0	1.41
(de França Viana, 2017)	Campus Ceres IFG, Goias	600	24.6	1601	70.0	5.36	Carioca	06/20/2015	80	163.5	510.1	336.8	4.21
							IPR Uirapuru	06/01/2016	80	193.1	544.2	368.7	4.61
(Schmidt and Valiati, 2006)	Cristalina, Goias	1000	20.5	1600	40.0	451.68	Carioca	07/13/2004	59	155.0	155.0	155.0	2.63
(Ferreira, 2015)	Paracatu, Minas Gerais	524	21.0	1453	72.0	29.60	Carioca	05/12/2015	59	390.7	390.7	390.7	6.62
						30.25	Carioca	06/10/2015	67	274.5	274.5	274.5	4.10

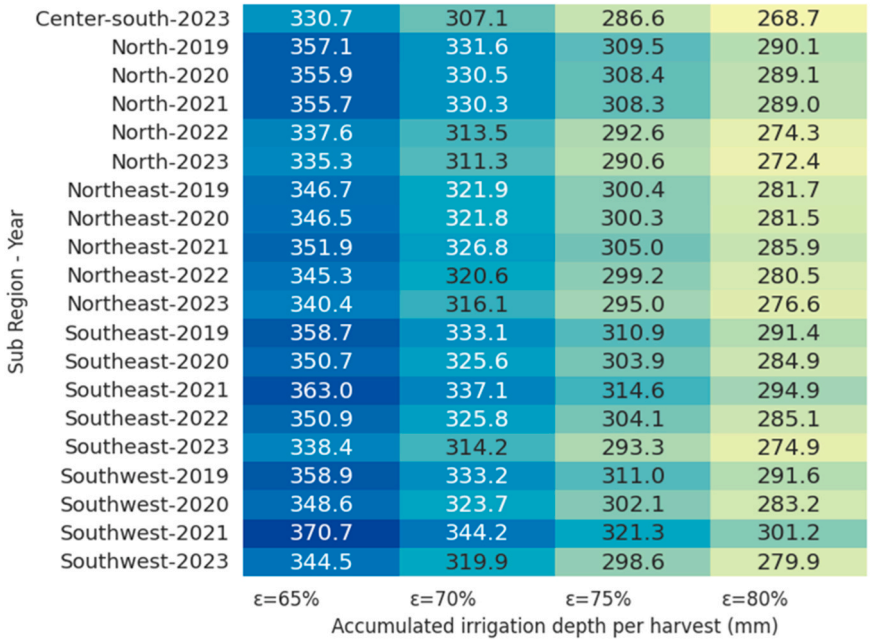

Fig. 11. Accumulated mean depth of crop water use for dry beans during the dry season, considering different application efficiency values for each year and sub-Region of Mato Grosso.

Fig. 12. a) Location of irrigated field with center pivot equipped with integrated monitoring and control units located in the municipality of Porto dos Gauchos in the North subregion of Mato Grosso. b) Center pivots with at least one year of dry bean harvest during the dry season.

depth applied per irrigation event can range from 5 to 10 mm. However, this often leads to applying more water than necessary, even considering the soil's water-holding capacity.

There are noticeable differences between crop water requirements and irrigation management practices. These differences lead to discrepancies in the monthly accumulated water depth, with an underestimation of water needs in May, June, and July and an overestimation in August. Although the overall trend of estimated water requirements by harvest aligns with the actual field data, there is a timing mismatch. The estimated water needed looks after the crop water requirement for its development, while field practices look after replenishing soil water capacity before the crop development despite the losses involved in the process.

Table 5 shows a comparison between the harvest accumulated water and phenologic metrics such as the start and end of the season. The estimated SOS differed by seven days in 2022 and six days in 2023. This might be due to the practice of delaying seedling to improve logistics at harvest time. The field EOS differed from the estimated by one and five days for 2022 and 2023, respectively. The results of start and end of the season estimated through the NDVI time series was favorable and congruent with in-field observations.

Looking at the total accumulated water by harvest, the estimated depth underestimates the water applied by 37.4 %5 and 31.4 %, respectively. Even though the current approach of estimating irrigation depth based on the crop water need does not follow the monthly irrigation practices, the accumulated depth under an efficiency of 65 % provides a good estimation by harvest season for water management purposes. It is important to mention that the efficiency of 65 % does not

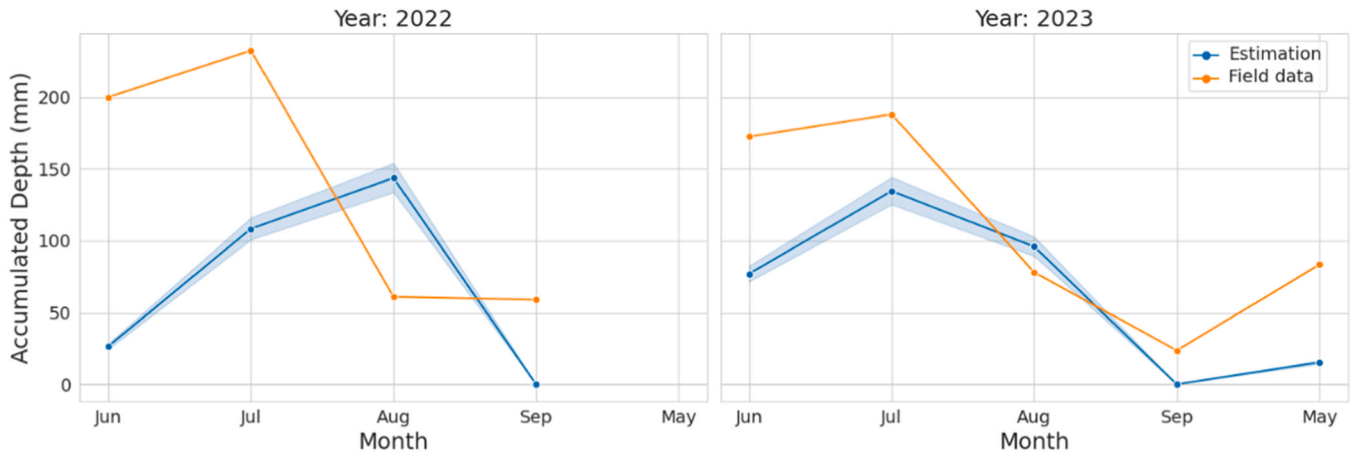

Fig. 13. Monthly accumulated water depth in mm by year. Estimated irrigation depth scenarios are represented with the blue shadow line. The upper and lower limit corresponds to water depth scenarios of 65 % and 80 % efficiency, respectively.

Table 5
Comparison of main parameters estimated in the study with field data.

Source	SOS date	SOS	EOS date	EOS	Accumulated depth (mm)
Field data	06/06/2022	157	08/31/2022	243	493.33
Field data	05/16/2023	136	08/25/2023	237	521.75
Estimation (ε=65 %)	06/13/2022	164	09/01/2022	244	308.87
Estimation (ε=65 %)	05/22/2023	142	08/30/2023	242	357.90

mean that the irrigation systems are inefficient, but numerically, it considers the surplus water needed to attend to the irrigation practices rather than the crop water need.

Field records from nineteen center pivots in Nova Ubirata, Sorriso, and Vera were provided by an irrigation consulting company. These records aided farm managers in optimizing water application. Monthly cumulative irrigation depths for the 2022 crop season were compared with the estimated irrigation (Fig. 14a-c), and their agreement was evaluated throughout the growing season (Fig. 14 d). In fields with more measurement equipment, discrepancies between estimated and reported irrigation depths were reduced. As shown in Fig. 13, there was an underestimation from May through July due to the practice of achieving field capacity. Although the estimated irrigation generally aligned with actual irrigation, there was a consistent underprediction, which was especially noticeable in August. The scatter plot (Fig. 14 d) reveals a strong positive correlation (R = 0.92) between reported and estimated irrigation, suggesting that the estimation model is fairly accurate. However, with a bias of −21.88 mm, the model tends to underpredict by an average of 21.88 mm, highlighting the need for model refinement to improve accuracy.

Comparing reported irrigation depths with estimated values revealed that a water efficiency scenario of ε = 65 % minimized errors. Table 6 presents the mean accumulated irrigation depths considering an application efficiency of ε = 65 %. The North, Northeast, and Southeast regions displayed relatively stable trends with minor fluctuations, while the Center-south and Southwest regions showed more variability and higher values in certain years. The mean irrigation depths for each year exhibited slight variations, with the highest mean recorded in 2021 (356.23 mm), coinciding with a later SOS. The median values were generally higher than the means, indicating a skewed distribution where higher values had more influence.

4.5. *Irrigation water use*

The irrigation water use (IWU) for each year was calculated at field scale by multiplying the water depth needed for the crop times the area of each center pivot. Table 7 shows the estimated IWU by subregion and for the state for the period of study. As it was mentioned before, most of the active center pivots with dry beans are in the North region, due to its favorable weather condition along the transition from the Cerrado to the Amazon biome. The North subregion accounts for 43 % of the total IWU of the state. Looking at the state level, there has been an increment in IWU in every year. Particularly, in 2020 there was a rise in 56 % compared to 2019, and 33 % in 2023 compared to 2022. It is estimated that the IWU for the third crop season of dry bean 2022/2023 was 604.42 million of cubic meters for the entire state of Mato Grosso; however, knowing that current irrigation practices apply more water than the crop needs for its developmental stage, it is likely that the total IWU could be higher.

Fig. 15 shows the IWU in millions of cubic meters for the state and

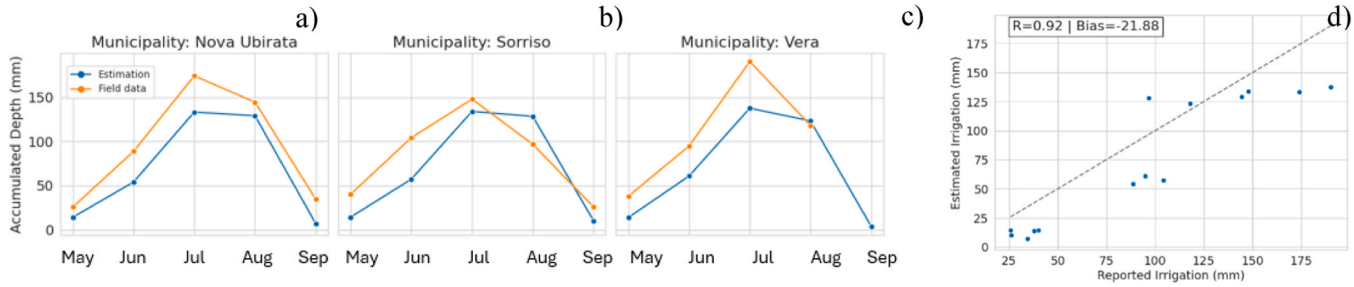

Fig. 14. Monthly accumulated water depth in mm by Municipality for year 2023 (Harvest 2022/2023). Estimated irrigation depth with ε=65 % is represented with the blue line.

Table 6
Accumulated mean irrigation depth (mm) with 65 % application efficiency by year and subregion.

Year	Harvest	Mato Grosso sub-regions					Total	
		Center-south	North	Northeast	Southeast	Southwest	Mean	Median
2019	2018/2019		357.1	346.68	358.69	358.86	356.59	358.86
2020	2019/2020		355.88	346.51	350.67	348.58	354.82	362.41
2021	2020/2021		355.68	351.92	362.99	370.69	356.23	370.69
2022	2021/2022		337.64	345.28	350.86		338.94	363.70
2023	2022/2023	330.71	335.27	340.37	338.37	344.54	335.99	356.17

Table 7
Total irrigation water use volume in millions of m^3 estimated for dry beans cultivated in center pivots during the dry season for years 2019–2023.

Year	Harvest	Center-south	North	Northeast	Southeast	Southwest	Mato Grosso
2019	2018/2019		98.89	6.23	8.35	0.05	227.02
2020	2019/2020		156.07	8.76	12.25	0.08	354.23
2021	2020/2021		180.00	8.42	19.22	0.41	415.70
2022	2021/2022		196.13	21.21	10.61		455.91
2023	2022/2023	2.28	253.86	31.02	16.03	0.31	604.42

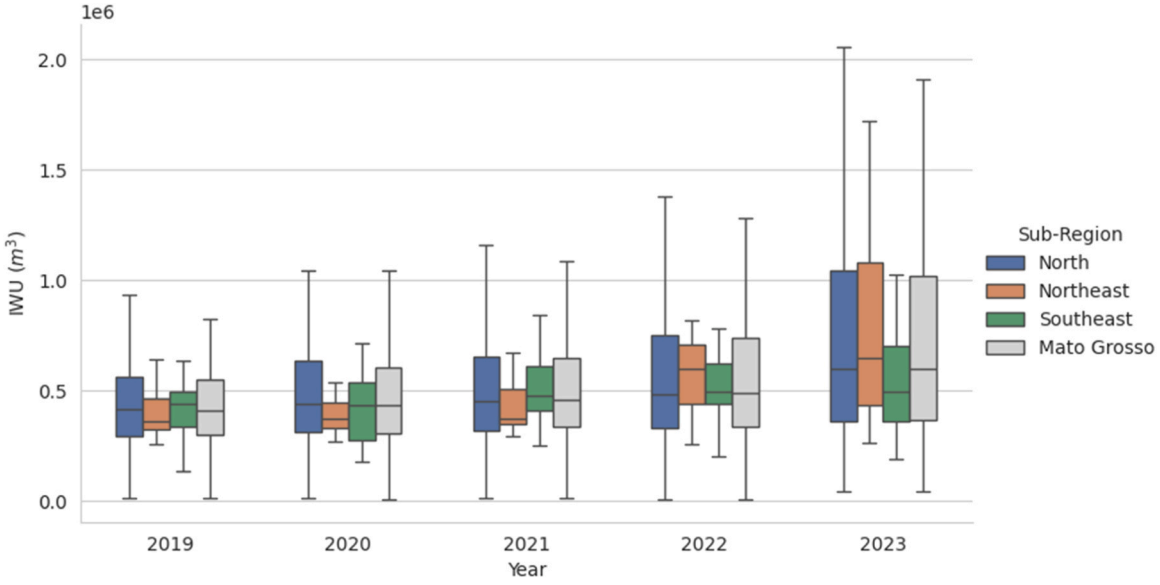

Fig. 15. Box plot of irrigation water use volume estimated for dry beans cultivated during the dry season for subregions with consecutive records throughout 2019–2023.

the North, Northeast, and Southeast subregions. The increment of the mean IWU by subregion is also seen in Fig. 15. Despite the high concentration of center pivot in the North region, for most of the year in the period of study, excepting for 2019, the mean IWU is below the state mean IWU. The Northeast and Southwest have a lower density of center pivots; however, they have a higher mean IWU than the North. In the Northeast, particularly for 2022 and 2023, the mean IWU is higher than the state mean IWU. The Southwest presented the highest mean IWU from 2019 to 2021. This means that the regional differences of IWU cannot be neglected in future studies, especially for potential expansions of irrigated fields.

4.6. Final considerations

Dry beans, a staple in the Brazilian diet, are essential for Brazil's food security. In recent years, the Cerrado Region, which accounts for 48 % of the agricultural land in the country, has adopted the third harvest, which consists of cultivating dry beans during the dry season (Fall and Winter) based mostly on an irrigation system to do so. Dry bean production during the third harvest has been consistent and is expected to rise despite current climate change trends. However, due to the large extension of the region, local variability of weather, and dynamic agricultural practices, the monitoring of IWU is challenging. Even though areas and yield of dry beans are reported months after the crop season's end, no official IWU numbers could promote water management planning. This study aimed to estimate the IWU of center pivots using remote sensing tools that can be applied by using free satellite products on open-source platforms like Google colab and Google Earth engine. The study focused on IWU of the dry season (third harvest) because of the high-water use compared to other seasons, thus being more vulnerable to water scarcity. The study was developed in the Brazilian state of Mato Grosso due to its highest development potential among other states in Cerrado.

A combination of remote sensing tools, such as the analysis of NDVI time series from Sentinel 2 A, were applied for the classification of crops, and the extraction of phenological parameters like SOS, EOS, and duration of the season were extracted using a customized version of xr_phenology function from DEA. Active pivot areas identified with dry beans matched official reports, with slight overestimations of 3.4 % and 15.2 % for 2022 and 2023, respectively. It was possible to identify the

most probable dates of SOS and EOS. However, it is recognized that SOS and EOS are subject to delays in the aims of improving the logistics of seedling and harvesting.

The irrigation requirement for individual fields was computed by applying the P-M method based on climate variables extracted from ERA5-Land. The water depth obtained with an application efficiency of 65 % provided the closest values to literature. Compared to field records, accumulated water depth applied by month based on the crop water needs could not capture the local irrigation practices. Current irrigation practices during the dry season consist of replenishing the soil to bring soil water capacity near to its field capacity while reducing water application during the mid and late season, when foliage area is high, to reduce the risk of plant diseases. The lack of soil water measurement tools in most fields and the dependence on irrigation system configuration and electricity rate schedules result in inefficient water application practices. The use of larger nozzles, while reducing pressure and energy consumption, allows for significant water application per event, ranging from 5 to 10 mm. However, this often leads to a mismatch between the water actually needed by crops and the water applied, resulting in underestimation in the early months (May to July) and overestimation in August. Despite similar overall water needs, field practices focus on replenishing soil water capacity rather than aligning precisely with crop development stages, highlighting a need for more precise irrigation management to minimize water wastage and optimize crop growth.

The analysis of irrigation water use (IWU) at a field scale confirms that the North subregion, which benefits from favorable weather conditions at the transition from the Cerrado to the Amazon biome, accounts for 43 % of the state's total IWU. Overall, there has been a yearly increase in IWU across the state, with a notable 56 % rise in 2020 compared to 2019 and a 33 % increase in 2023 compared to 2022. For the third harvest of dry beans in 2022/2023, the IWU for Mato Grosso was estimated at 604.42 million cubic meters, potentially reaching more than that due to irrigation overuse. Despite the high concentration of center pivots in the North, its mean IWU is generally below the state average, except in 2019. In contrast, despite having fewer center pivots, the Northeast and Southeast regions exhibit higher mean IWU, with the Southeast leading from 2019 to 2021 and the Northeast exceeding the state mean IWU in 2022 and 2023. These regional variations highlight the importance of considering IWU differences in future studies, especially for potential irrigation expansions.

Besides the irrigation depth estimation, the current study also provided a recurrence pattern of irrigated field usage, providing a foundation for making informed predictions about future usage. By analyzing historical trends, identifying consistent and sporadic usage, and incorporating these insights into predictive models, stakeholders can make better strategic decisions, allocate resources more efficiently, and manage risks more effectively. Moreover, an updated map of center pivots in Mato Grosso was generated with data from ANA and MapBiomas, displaying information on field usage, biome, and mean theoretical water depth applied.

Due to the lack of detailed field data, often restricted for privacy reasons or simply not measured, the pivot performance characteristics, including application efficiency and operational timeframes, were estimated based on literature coefficients. The irrigation schedules were assumed to align with the lowest electricity costs in rural areas. Additionally, soil characteristics, such as daily moisture content and texture, posed constraints on accurately calculating effective rainfall. Due to the sparse network of meteorological stations, often located far from irrigated fields and with incomplete data, it was not possible to validate and calibrate the estimated crop evapotranspiration (ETc) with ground observations. Although many large farms have meteorological stations, these records are typically not publicly accessible. While this study highlights trends of over- and under-irrigation in large areas, distinguishing and quantifying the extent of water wastage will require more detailed ground-based measurements.

5. Conclusions

This study provided valuable insights into irrigation water use (IWU) in Mato Grosso's dry season (third harvest) using remote sensing tools. Despite challenges in monitoring IWU due to regional variability and dynamic agricultural practices, the study estimated IWU with reasonable accuracy. Findings indicate significant regional differences in IWU, with the North subregion accounting for a substantial portion of the state's total IWU. Annual increases in IWU highlight the need for efficient water management practices. For the third dry bean harvest in 2022/2023, the IWU for Mato Grosso was estimated at 604.42 million cubic meters, with a yearly increase in IWU observed for dry bean cultivation during the dry season. Current irrigation practices often misalign with crop water needs, underscoring the importance of precise irrigation management. Crop water demand patterns differ from the theoretical FAO approach, largely due to the intense three-crop dynamic, revealing that practical irrigation deviates from theoretical assumptions. The study also offered a recurrence pattern of irrigated field usage, aiding future usage predictions and strategic decision-making.

The irrigation depth retrieval proposed in this study provided a fair estimate for the dry season, providing a cost-effective method to estimate Irrigation Water Use (IWU) over large areas in almost real-time. This data is crucial for municipal and state water management, especially when planning for future scenarios with extended dry seasons, which can intensify tensions among water users due to the Cerrado's characteristics of low flow and frequent wildfires. Nevertheless, additional modifications could improve the outcome. For instance, if crop records of center pivots were available, it would be possible to apply more advanced machine learning tools, such as random forest, to classify crops at a larger scale with more accuracy. Discrepancies between practical and theoretical approaches were mostly tied to irrigation application efficiency (ε). However, future work, supported by extensive field and meteorological data, should reassess the crop coefficient (Kc) and possible adjustments of Kc for dry beans and other crops during the dry season to better reflect real farm conditions. Detailed studies on staggered planting and internal pivot dynamics are needed to refine water management practices, and examining their effect on yield could optimize irrigation practices, particularly in seasons when rainfall is delayed. Alternatively, the Penman-Monteith approach could be extracted from local models adapted to the Brazilian morphoclimatic reality (de Sousa Junior et al., 2022), such as the Operational Simplified Surface Energy Balance model (SSEBop-Br). Moreover, radar products such as Sentinel 1 SAR could be used to quantify the overuse of water in fields. Improved irrigation depth estimation and the incorporation of advanced tools and local models could further enhance accuracy, supporting sustainable agricultural practices in Brazil's key agricultural regions.

Declaration of Competing Interest

The authors declare that they have no known competing financial interests or personal relationships that could have appeared to influence the work reported in this paper.

Acknowledgments

The authors express their sincere gratitude to Thales André Rodrigues de Souza from Agir Agronegócios LTDA for generously providing the valuable field data, which was instrumental to this study. We also extend our appreciation to Professor Fabio Marin for his insightful feedback and thoughtful suggestions, which significantly contributed to the improvement of this work. Any opinions, findings, and conclusions or recommendations expressed in this paper are those of the authors and do not necessarily reflect the views of the University of Sao Paulo.

Appendix A. Supporting information

Supplementary data associated with this article can be found in the online version at doi:10.1016/j.agwat.2024.109128.

Data availability

Data will be made available on request.

References

de Abreu, M.J., Leite, M.E., Ferreira, A.N., Pereira, R., Pereira, F.A.C., et al., 2022. Resistance of common bean lines to Sclerotinia sclerotiorum isolates under different environmental conditions. Pesqui. Agropecu. Bras. 57. https://doi.org/10.1590/S1678-3921.PAB2022.V57.02877.

de Albuquerque, A.O., de Carvalho, O.A., de Carvalho, O.L.F., de Bem, P.P., Guimarães Ferreira, P.H., et al., 2020. Deep semantic segmentation of center pivot irrigation systems from remotely sensed data. Remote Sens (Basel) 12 (13). https://doi.org/10.3390/rs12132159.

Ali, M., Mubarak, S., 2017. Effective Rainfall Calculation Methods for Field Crops: An Overview, Analysis and New Formulation. Asian Res. J. Agric. 7 (1), 1–12. https://doi.org/10.9734/arja/2017/36812.

Allen, R.G., 2000. Using the FAO-56 dual crop coefficient method over an irrigated region as part of an evapotranspiration intercomparison study. J. Hydrol. (Amst.) 229 (1–2), 27–41. https://doi.org/10.1016/S0022-1694(99)00194-8.

Allen, R.G., Tasumi, M., Trezza, R., 2006. Why Use Reference Evapotranspiration to Calibrate Satellite-Based Energy Balances? World Environmental and Water Resource Congress 2006. American Society of Civil Engineers, Reston, VA, pp. 1–12.

Althoff, D., Rodrigues, L.N., 2019. The expansion of center-pivot irrigation in the cerrado biome. Irriga 1 (1IagriSpecialEdition), 56–61. https://doi.org/10.15809/irriga.2019v1n1p56-61.

Althoff, D., Rodrigues, L.N., da Silva, D.D., 2021. Assessment of water availability vulnerability in the Cerrado. Appl. Water Sci. 11 (11), 1–14. https://doi.org/10.1007/s13201-021-01521-2.

ANA. 2019a. Manual dos Usos Consuntivos de Água do Brasil.

ANA. 2019b. Atlas Irrigação: Coeficientes técnicos de uso da água para a agricultura irrigada. Brasília.

ANA. 2021. Atlas Irrigação. Uso da água na agricultura irrigada 2° EDIÇÃO.

Arvor, D., Dubreuil, V., Ronchail, J., Simões, M., Funatsu, B.M., 2014. Spatial patterns of rainfall regimes related to levels of double cropping agriculture systems in Mato Grosso (Brazil). Int. J. Climatol. 34 (8), 2622–2633. https://doi.org/10.1002/joc.3863.

Bégué, A., Arvor, D., Bellon, B., Betbeder, J., de Abelleyra, D., et al., 2018. Remote sensing and cropping practices: A review. Remote Sens (Basel) 10 (1). https://doi.org/10.3390/rs10010099.

Bigolin, T., Talamini, E., 2024. Impacts of climate change scenarios on the corn and soybean double-cropping system in Brazil. Climate 12 (3), 1–21. https://doi.org/10.3390/cli12030042.

Brocca, L., Tarpanelli, A., Filippucci, P., Dorigo, W., Zaussinger, F., et al., 2018. How much water is used for irrigation? A new approach exploiting coarse resolution satellite soil moisture products. Int. J. Appl. Earth Obs. Geoinf. 73 (May), 752–766. https://doi.org/10.1016/j.jag.2018.08.023.

Brown, J.C., Kastens, J.H., Coutinho, A.C., Victoria, D. de C., Bishop, C.R., 2013. Classifying multiyear agricultural land use data from Mato Grosso using time-series MODIS vegetation index data. Remote Sens Environ. 130, 39–50. https://doi.org/10.1016/j.rse.2012.11.009.

Cherubin, M.R., M. Lustosa Carvalho, B. da Silva Vanolli, B. Schiebelbein, D. Aquino de Borba, et al. 2022. Guia prático de plantas de cobertura: aspectos fitotécnicos e impactos sobre a saúde do solo. Universidade de São Paulo - USP.

Colman, C.B., Guerra, A., Roque, F. de O., Rosa, I.M.D., Oliveira, P.T.S. de, 2022. Identifying priority regions and territorial planning strategies for conserving native vegetation in the Cerrado (Brazil) under different scenarios of land use changes. Sci. Total Environ. 807. https://doi.org/10.1016/j.scitotenv.2021.150998.

Colussi, J., Schnitkey, G., Paulson, N., 2023. Will Brazil Emerge as the Number One Corn Exporting Nation? Farm. Dly. 13 (48), 1–5.

Conab. 2022. Calendário de Plantio e Colheita de Grãos no Brasil 2022. Conab: 1–76.

Conab, 2023. Acompanhamento da safra brasileira: Grãos, décimo segundo levantamento 2022/23. Conab - Cia. Nac. De. Abast. 10, 1–111.

CONAB. 2016. Perspectivas de diversificação e de investimentos na produção de arroz - trigo - feijão. Brasília.

Cruz, T.T., Asmus, G.L., Garcia, R.A., 2020. Crotalaria species in succession to soybean for the management of Pratylenchus brachyurus. Cienc. Rural 50 (7), 1–8. https://doi.org/10.1590/0103-8478cr20190645.

D'Odorico, P., Gonsamo, A., Gough, C.M., Bohrer, G., Morison, J., et al., 2015. The match and mismatch between photosynthesis and land surface phenology of deciduous forests. Agric. Meteor. 214–215 25–38. https://doi.org/10.1016/j.agrformet.2015.07.005.

van der Maaten, L., Hinton, G., 2008. Visualizing data using t-SNE. J. Mach. Learn. Res. 219, 2579–2605.

Developers, X. 2014. Xarray documentation. https://docs.xarray.dev/en/stable/user-guide/data-structures.html (accessed 1 October 2023).

Duarte, Y.C.N., Sentelhas, P.C., 2020. NASA/POWER and DailyGridded weather datasets—how good they are for estimating maize yields in Brazil? Int J. Biometeorol. 64 (3), 319–329. https://doi.org/10.1007/s00484-019-01810-1.

DW Brasil. 2024. Os impactos esperados da seca prolongada no Brasil. UOL Cultura. https://cultura.uol.com.br/noticias/dw/70216914_os-impactos-esperados-da-seca-prolongada-no-brasil.html (accessed 13 October 2024).

FAO. 2020. Land use in agriculture by the numbers. Food and Agriculture Organization of the United Nations News. https://www.fao.org/sustainability/news/detail/en/c/1274219/ (accessed 11 April 2022).

Ferrarini, A. dos S.F., J.B. de S. Ferreira Filho, S.V. Cuadra, D. de C. Victoria, and M. Horridge. 2019. The Expansion of Irrigated Agriculture in Brazil and Potential Regional Limitations.: 139–157. doi: 10.1007/978-981-13-6101-2_7.

Ferreira, F.E.P. 2015. Uso do software intecperímetro® na avaliação do manejo da irrigação nas culturas do milho e feijão.

Ferreira, F.L.V., Rodrigues, L.N., Althoff, D., Amorim, R.S.S., 2023. Spatial–Temporal Variability of Climatic Water Balance in the Brazilian Savannah Region River Basins. Water (Switz.) 15 (10), 1–16. https://doi.org/10.3390/w15101820.

Folhes, M.T., Rennó, C.D., Soares, J.V., 2009. Remote sensing for irrigation water management in the semi-arid Northeast of Brazil. Agric. Water Manag 96 (10), 1398–1408. https://doi.org/10.1016/j.agwat.2009.04.021.

de França Viana, T. 2017. Aspecto produtivo da cultura do feijoeiro sob diferentes lâminas via pivô central Aspecto produtivo da cultura do feijoeiro sob diferentes lâminas via pivô central.

Francisco, E.A.B., Kappes, C., 2012. Cerrado brasileiro carece de mais investimentos em práticas sustentáveis. Vis. ão Agr. ícola 10, 55–57.

Frizzone, J.A., Rezende, R., Camargo, A.Pires, Colombo, Antonio, 2018. Irrigação por Aspersão. UEM.

Gascon, F., Bouzinac, C., Thépaut, O., Jung, M., Francesconi, B., et al., 2017. Copernicus Sentinel-2A calibration and products validation status. Remote Sens (Basel) 9 (6). https://doi.org/10.3390/rs9060584.

Geng, L., Ma, M., Wang, X., Yu, W., Jia, S., et al., 2014. Comparison of eight techniques for reconstructing multi-satellite sensor time-series NDVI data sets in the heihe river basin, China. Remote Sens (Basel) 6 (3), 2024–2049. https://doi.org/10.3390/rs6032024.

Geoscience Australia. 2024. DEA tools: Temporal. Digital Earth Australia Knowledge Base. Vegetation Phenology. https://knowledge.dea.ga.gov.au/notebooks/Tools/gen/dea_tools.temporal/ (accessed 3 April 2023).

Gorelick, N., Hancher, M., Dixon, M., Ilyushchenko, S., Thau, D., et al., 2017. Google Earth Engine: Planetary-scale geospatial analysis for everyone. Remote Sens Environ. 202, 18–27. https://doi.org/10.1016/j.rse.2017.06.031.

Guzinski, R., Nieto, H., Ramo Sánchez, R., Sánchez, J.M., Jomaa, I., et al., 2023. Improving field-scale crop actual evapotranspiration monitoring with Sentinel-3, Sentinel-2, and Landsat data fusion. Int. J. Appl. Earth Obs. Geoinf. 125. https://doi.org/10.1016/j.jag.2023.103587.

Hayasaka, S. 2022. How Many Clusters? Methods for choosing the right number of clusters. Medium. https://towardsdatascience.com/how-many-clusters-6b3f220f0ef5.

Heinemann, A.B., Ramirez-Villegas, J., Souza, T.L.P.O., Didonet, A.D., di Stefano, J.G., et al., 2016. Drought impact on rainfed common bean production areas in Brazil. Agric. Meteor. 225, 57–74. https://doi.org/10.1016/j.agrformet.2016.05.010.

Hersbach, H. 2016. The ERA5 Atmospheric Reanalysis. AGU fall meeting abstracts. p. NG33D–01.

Hird, J.N., McDermid, G.J., 2009. Noise reduction of NDVI time series: An empirical comparison of selected techniques. Remote Sens Environ. 113 (1), 248–258. https://doi.org/10.1016/j.rse.2008.09.003.

Irmak, S., L. Odhiambo, W. Kranz, and D. Eisenhauer. 2011. Irrigation Efficiency and Uniformity, and Crop Water Use Efficiency.

Jalilvand, E., Tajrishy, M., Ghazi Zadeh Hashemi, S.A., Brocca, L., 2019. Quantification of irrigation water using remote sensing of soil moisture in a semi-arid region. Remote Sens Environ. 231 (August 2018), 111226. https://doi.org/10.1016/j.rse.2019.111226.

Ji, Z., Pan, Y., Zhu, X., Wang, J., Li, Q., 2021. Prediction of crop yield using phenological information extracted from remote sensing vegetation index. Sens. (Switz.) 21 (4), 1–17. https://doi.org/10.3390/s21041406.

Kuchler, P.C., Bégué, A., Simões, M., Gaetano, R., Arvor, D., et al., 2020. Assessing the optimal preprocessing steps of MODIS time series to map cropping systems in Mato Grosso, Brazil. Int. J. Appl. Earth Obs. Geoinf. 92 (April). https://doi.org/10.1016/j.jag.2020.102150.

Lewis, K., de, F., Barros, V., Cure, M.B., Davies, C.A., Furtado, M.N., et al., 2022. Mapping native and non-native vegetation in the Brazilian Cerrado using freely available satellite products. Sci. Rep. 12 (1). https://doi.org/10.1038/s41598-022-05332-6.

Linderman, G.C., Steinerberger, S., 2019. Clustering with t-SNE, Provably. SIAM J. Math. Data Sci. 1 (2), 313–332. https://doi.org/10.1137/18M1216134.

Ma, C., Johansen, K., McCabe, M.F., 2022. Monitoring Irrigation Events and Crop Dynamics Using Sentinel-1 and Sentinel-2 Time Series. Remote Sens (Basel) 14 (5), 1–21. https://doi.org/10.3390/rs14051205.

Marin, F.R., Angelocci, L.R., Nassif, D.S.P., Vianna, M.S., Pilau, F.G., et al., 2019. Revisiting the crop coefficient–reference evapotranspiration procedure for improving irrigation management. Theor. Appl. Clim. 138 (3–4), 1785–1793. https://doi.org/10.1007/s00704-019-02940-7.

Massari, C., Modanesi, S., Dari, J., Gruber, A., De Lannoy, G.J.M., et al., 2021. A review of irrigation information retrievals from space and their utility for users. Remote Sens (Basel) 13 (20), 1–26. https://doi.org/10.3390/rs13204112.

Muñoz-Sabater, J., Dutra, E., Agustí-Panareda, A., Albergel, C., Arduini, G., et al., 2021. ERA5-Land: A state-of-the-art global reanalysis dataset for land applications. Earth Syst. Sci. Data 13 (9), 4349–4383. https://doi.org/10.5194/essd-13-4349-2021.

do Nascimento Bendini, H., Garcia Fonseca, L.M., Schwieder, M., Sehn Körting, T., Rufin, P., et al., 2019. Detailed agricultural land classification in the Brazilian cerrado based on phenological information from dense satellite image time series. Int. J. Appl. Earth Obs. Geoinf. 82 (June)), 101872. https://doi.org/10.1016/j.jag.2019.05.005.

Noronha Marcuzzo, F.F., Lima Oliveira, N.De, Dias Cardoso, M.R., 2012. Tendência do número de dias de chuva no estado do Mato Grosso Trend in Number of Days of Precipitation in the State of Mato Grosso. Ciência e Nat. 34 (2), 59–82. ⟨https://www.proquest.com/openview/399dea3b08cbc62a186e695122cfecd7/1?pq-origsite=gscholar&cbl=2034996⟩ (accessed 15 September 2024).

de Oliveira, H.F.E., de Castro, L.E.V., Sousa, C.M., Alves Júnior, L.R., Mesquita, M., et al., 2024. Geotechnologies in Biophysical Analysis through the Applicability of the UAV and Sentinel-2A/MSI in Irrigated Area of Common Beans: Accuracy and Spatial Dynamics. Remote Sens (Basel) 16 (7). https://doi.org/10.3390/rs16071254.

Osti, A.M., Dallacort, R., Tieppo, R.C., Grzebieluckas, C., Conceição, A.M., 2019. Rentabilidade do milho e do feijão submetido a diferentes lâminas de irrigação em Mato Grosso. Rev. De. Econ. e Sociol. Rural 57 (4), 505–518. https://doi.org/10.1590/1806-9479.2019.186329.

Peña-Arancibia, J.L., McVicar, T.R., Paydar, Z., Li, L., Guerschman, J.P., et al., 2014. Dynamic identification of summer cropping irrigated areas in a large basin experiencing extreme climatic variability. Remote Sens Environ. 154, 139–152. https://doi.org/10.1016/j.rse.2014.08.016.

Pereira Guimarães, D., Landau, E.C., Henriques Fontenelle, T., 2023. Agricultura Irrigada por Pivôs Centrais no Brasil. Cat. De. Metadados da ANA. ⟨https://metadados.snirh.gov.br/geonetwork/srv/api/records/e2d38e3f-5e62-41ad-87ab-990490841073⟩.

Pimenta, F.M., Speroto, A.T., Costa, M.H., Dionizio, E.A., 2021. Historical changes in land use and suitability for future agriculture expansion in Western Bahia, Brazil. Remote Sens (Basel) 13 (6), 1–31. https://doi.org/10.3390/rs13061088.

Poličar, P. 2023. openTSNE: Extensible, parallel implementations of t-SNE. GitHub. https://opentsne.readthedocs.io/en/latest/index.html.

Pousa, R., Costa, M.H., Pimenta, F.M., Fontes, V.C., Castro, M., 2019. Climate change and intense irrigation growth in Western Bahia, Brazil: The urgent need for hydroclimatic monitoring. Water (Switz.) 11 (5). https://doi.org/10.3390/w11050933.

Rattis, L., Brando, P.M., Macedo, M.N., Spera, S.A., Castanho, A.D.A., et al., 2021. Climatic limit for agriculture in Brazil. Nat. Clim. Chang 11 (12), 1098–1104. https://doi.org/10.1038/s41558-021-01214-3.

Rodigheri, G., Sanches, I.D., Richetti, J., Tsukahara, R.Y., Lawes, R., et al., 2023. Estimating Crop Sowing and Harvesting Dates Using Satellite Vegetation Index: A Comparative Analysis. Remote Sens (Basel) 15 (22). https://doi.org/10.3390/rs15225366.

Rogers, D.H., J. Aguilar, I. Kisekka, and F.R. Lamm. 2017. Center pivot irrigation system losses and efficiency. Proceedings of the 29th Annual Central Plains Irrigation Conference, Burlington, Colorado, Feb.21-22 (March): 19–34.

Rolle, M., Tamea, S., Claps, P., 2021. ERA5-based global assessment of irrigation requirement and validation. PLoS One 16 (4 April), 1–21. https://doi.org/10.1371/journal.pone.0250979.

Rudorff, B., and L. Oliveira. 2023. MapBiomas General “Handbook”. Irrigation - Appendix.

Running, S.W., Q. Mu, M. Zhao, and A. Moreno. 2024. User’s Guide MODIS Global Terrestrial Evapotranspiration (ET) Product (MOD16A2/A3 and Year-end Gap-filled MOD16A2GF/A3GF) NASA Earth Observing System MODIS Land Algorithm (For Collection 6.1).

Santos, A.B., Costa, M.H., Mantovani, E.C., Boninsenha, I., Castro, M., 2020. A remote sensing diagnosis of water use and water stress in a region with intense irrigation growth in brazil. Remote Sens (Basel) 12 (22), 1–16. https://doi.org/10.3390/rs12223725.

Schmidt, É.W., Valiati, M.I., 2006. Avaliação do manejo de irrigação para a cultura de feijão (Phaseolus vulgaris) irrigada por pivô central na agricola Wehrmann em Cristalina-GO. Campo Digit. 1 (1), 23–31.

Service/ECMWF, C.C.C. 2023. Fact sheet: Reanalysis. https://www.ecmwf.int/en/about/media-centre/focus/2023/fact-sheet-reanalysis.

Silva, J.F., Flake, O., 2019. Brazilian dry bean production. USDA Foreign Agicultural Serv. 1–6.

Silva, J.L.B. da, Moura, G.B. de A., Silva, M.V. da, Oliveira-Júnior, J.F. de, Jardim, A.M. da R.F., et al., 2023. Environmental degradation of vegetation cover and water bodies in the semiarid region of the Brazilian Northeast via cloud geoprocessing techniques applied to orbital data. J. South Am. Earth Sci. 121. https://doi.org/10.1016/j.jsames.2022.104164.

Silva, J.L.B. da, Silva, M.V. da, Jardim, A.M. da R.F., Lopes, P.M.O., Oliveira, H.F.E. de, et al., 2024. Geospatial Insights into Aridity Conditions: MODIS Products and GIS Modeling in Northeast Brazil. Hydrology 11 (3). https://doi.org/10.3390/hydrology11030032.

Silva, M.V. da, Pandorfi, H., Oliveira-Júnior, J.F. de, Silva, J.L.B. da, Almeida, G.L.P. de, et al., 2022. Remote sensing techniques via Google Earth Engine for land degradation assessment in the Brazilian semiarid region, Brazil. J. South Am. Earth Sci. 120. https://doi.org/10.1016/j.jsames.2022.104061.

da Silva, O.F., and A.E. Wander 2018. Caracterização e avaliação econômica do sistema de cultivo de feijão-comum irrigado no Cerrado o caso da cultivar BRS Estilo. Caracterização e avaliação econômica de sistemas de produção e cultivo de grãos em biomas brasileiros. Embrapa, Brasilia, DF. p. 47–68.

da Silva Tavares, P., Acosta, R., Nobre, P., Resende, N.C., Chou, S.C., et al., 2023. Water balance components and climate extremes over Brazil under 1.5 °C and 2.0 °C of global warming scenarios. Reg. Environ. Change 23 (1). https://doi.org/10.1007/s10113-023-02042-1.

Singer, M.B., Asfaw, D.T., Rosolem, R., Cuthbert, M.O., Miralles, D.G., et al., 2021. Hourly potential evapotranspiration at 0.1° resolution for the global land surface from 1981-present. Sci. Data 8 (1), 1–13. https://doi.org/10.1038/s41597-021-01003-9.

Soares, M.B., De Lima, J.P., Freddi, O.D.S., Tavanti, T.R., Tavanti, R.F.R., 2019. Desempenho De Cultivares De Feijoeiro Irrigado No Ecótono Cerrado-Amazônia. Nativa 7 (3), 244. https://doi.org/10.31413/nativa.v7i3.6494.

Song, X.P., Huang, W., Hansen, M.C., Potapov, P., 2021. An evaluation of Landsat, Sentinel-2, Sentinel-1 and MODIS data for crop type mapping. Sci. Remote Sens. 3. https://doi.org/10.1016/j.srs.2021.100018.

de Sousa Junior, M.F., Fonseca, L.M.G., Bendini, H. do N., 2022. Estimation of water use in center pivot irrigation using evapotranspiration time series derived by landsat: a study case in a Southeastern Region of the Brazilian Savanna. Remote Sens (Basel) 14 (23), 5929. https://doi.org/10.3390/rs14235929.

Stamford, J.D., Vialet-Chabrand, S., Cameron, I., Lawson, T., 2023. Development of an accurate low cost NDVI imaging system for assessing plant health. Plant Methods 19 (1). https://doi.org/10.1186/s13007-023-00981-8.

USGS. 2018. Methods for Deriving Metrics. https://www.usgs.gov/special-topics/remote-sensing-phenology/science/methods-deriving-metrics#overview (accessed 3 September 2024).

Viovy, N., Arino, O., Belward, A.S., 1992. The Best Index Slope Extraction (BISE): A method for reducing noise in NDVI time-series. Int J. Remote Sens 13 (8), 1585–1590. https://doi.org/10.1080/01431169208904212.

Wander, A.E., 2007. Produção e consumo de feijão no Brasil, 1975-2005. Inf. ções Econ. ômicas.

WWF-Brasil. 2024. Amazon, Cerrado and Pantanal break new wildfire records in September. https://www.wwf.org.br/?89841/Amazon-Cerrado-and-Pantanal-break-new-wildfire-records-in-September (accessed 13 October 2024).

Zaussinger, F., Dorigo, W., Gruber, A., Tarpanelli, A., Filippucci, P., et al., 2019. Estimating irrigation water use over the contiguous United States by combining satellite and reanalysis soil moisture data. Hydrol. Earth Syst. Sci. 23 (2), 897–923. https://doi.org/10.5194/hess-23-897-2019.

Zhang, M., Abrahao, G., Cohn, A., Campolo, J., Thompson, S., 2021. A MODIS-based scalable remote sensing method to estimate sowing and harvest dates of soybean crops in Mato Grosso, Brazil. Heliyon 7 (7), e07436. https://doi.org/10.1016/j.heliyon.2021.e07436.